Immunolocalization of the Cellular *src* Protein in Interphase and Mitotic NIH c-*src* Overexpresser Cells

Thérèse David-Pfeuty and Yolande Nouvian-Dooghe

Institut Curie-Biologie, Centre Universitaire, 91405-Orsay Cedex, France

Abstract. The mouse mAb, mAb 327, that recognizes specifically both pp60^{v-src} and pp60^{c-src} in a wide variety of cells, has been used to determine precisely the various locations of pp60^{c-src} in NIH c-*src* overexpresser cells, using the technique of immunofluorescence microscopy. In interphase cells, the protein exhibits two main distributions: one that appears uniform and in association with the cell surface and the other that is patchy and juxtanuclear and coincides with the centrosomes. The juxtanuclear aggregation of pp60^{c-src}-containing patches depends on microtubules and does not seem to occur within the Golgi apparatus and the rough ER. At the G2-to-M-phase transition, a drastic change in the localization patterns of pp60^{c-src} takes place.

We also report experiments in which the NIH c-*src* overexpresser cells were exposed to Con A for various times to induce a redistribution of the cell surface Con A receptors. We show that, at each stage of the Con A–mediated endocytotic process, the Con A–receptor

complexes redistribute into structures to which pp60^{c-src} appears also to be associated: at first, into patches that form at the cell surface level and then, into a cap that stands at the cell center in a juxtanuclear position and that coincides with the Golgi apparatus. During this capping process, pp60^{c-src}-containing vesicles continue to accumulate in a centriolar spot, as in interphase, Con A-untreated cells, from which Con A is excluded.

The significance of the intracellular locations of pp60^{c-src} to the possible functions of the protein is discussed. Also, the distribution patterns of the cellular protein in the NIH c-*src* overexpresser cells are compared with those of pp60^{v-src} in RSV-transformed cells. The differences observed are discussed in relation with the differences in transforming capacities of the two proteins. Finally, the possible physiological significance of the association between pp60^{c-src} and the structures generated after the binding of Con A to its surface receptors is addressed.

D ETAILED studies of both the biochemistry and the localization of pp60^{v-src}, the transforming protein of RSV, have been possible owing to the availability of antisera of various origins, such as antisera from tumor-bearing rabbits (TBRs),[1] antisera against synthetic peptides corresponding to different domains of the molecule, and antisera against bacterially produced pp60^{v-src} (review in Parsons et al., 1984). Together, the results using these sera underline the fact that a majority of the pp60^{v-src} molecules produced in RSV-transformed, cultured cells exists in association with the cytoplasmic face of the plasma membrane (Willingham et al., 1979), particularly within the nonionic, detergent-insoluble cytoskeletal matrix (Burr et al., 1980), in adhesion plaques, "rosettes" (Rohrschneider, 1979; Nigg et al., 1982) and at intercellular contacts (Krueger et al., 1980). Moreover, a substantial amount of pp60^{v-src} has been found in intracellular structures that associate with the nu-

clear membranes via hydrophobic interactions (Resh and Erikson, 1985). Finally, pp60^{v-src} molecules that form a soluble cytoplasmic complex with two cellular proteins, pp50 and pp90, have been detected and are thought to represent a form of the protein, in transit to the plasma membrane (Brugge et al., 1983).

Most of the sera that recognize pp60^{v-src}, also recognize its cellular homologue, pp60^{c-src}. Therefore, the tools to study pp60^{c-src} exist. Yet, pp60^{c-src} in normal cultured cells is 50–100-fold less abundant than pp60^{v-src} in most RSV-transformed cells (Hunter and Sefton, 1980). This quantitative parameter has impeded studies of the cellular protein and consequently prevented a complete inventory of the differences that distinguish pp60^{v-src} from pp60^{c-src}. Like its viral counterpart, the cellular src protein belongs to the tyrosine protein kinase family (review in Jove and Hanafusa, 1987). Biochemical studies have taken advantage of this property and have provided information on pp60^{c-src}: the cellular *src* protein preferentially associates with plasma membranes, like pp60^{v-src}, although, contrary to pp60^{v-src}, such an interaction does not appear to occur via the non-

---

1. *Abbreviations used in this paper*: MTOC, microtubule organizing center; TBR, tumor-bearing rabbits; TRITC, tetramethyl rhodamine isothiocyanate.

ionic, detergent-insoluble cellular matrix (Loeb et al., 1987; Hamaguchi and Hanafusa, 1987); $pp60^{c\text{-}src}$ has been detected in intracellular membranes associated with the nuclear envelope, like $pp60^{v\text{-}src}$ (Resh and Erikson, 1985) and with more specific structures such as chromaffin granules (Parsons and Greutz, 1986) and synaptic vesicles (Barnekow et al., 1990); platelets have also been shown to contain a relatively high level of $pp60^{c\text{-}src}$ (Rendu et al., 1989; Ferrell et al., 1990); the cellular protein does not seem to form a soluble cytoplasmic complex with two cellular proteins, contrary to $pp60^{v\text{-}src}$ (Tamura et al., 1984).

Cell lines have been obtained that overexpress the cellular *src* protein after transfection with plasmids containing the c-*src* coding sequence (Iba et al., 1984; Parker et al., 1984; Shalloway et al., 1984; Johnson et al., 1985; Warren et al., 1988). Examination of the effects of overexpression of $pp60^{c\text{-}src}$ up to a level comparable to that of $pp60^{v\text{-}src}$ in RSV-transformed cells, has permitted the demonstration that qualitative differences between the viral and the cellular *src* proteins must be responsible for the induction of full cellular transformation and in vivo tumorigenicity.

The aim of the work presented in the first part of this article was to determine the probable intracellular location(s) of $pp60^{c\text{-}src}$ in normal cells by using $pp60^{c\text{-}src}$ overexpresser cells, the NIH (pM c-*src*/focus)B cells (Shalloway et al., 1984), in which the detection of the protein by immunofluorescence microscopy is possible. We also wanted to compare the localization of $pp60^{v\text{-}src}$ and $pp60^{c\text{-}src}$ in cells where the two proteins are expressed at a nearly equivalent level. Such a study, indeed, should help to identify intracellular targets for which the two proteins have a nearly similar or, on the contrary, a widely different affinity. Our observations indicate that the main features of the distribution patterns of the two proteins are rather different. In particular, a localization of $pp60^{c\text{-}src}$ similar to the most characteristic one of $pp60^{v\text{-}src}$, inside focal adhesion plaques and rosettes (Rohrschneider, 1980; Nigg et al., 1982) never appears. In the c-*src* overexpresser cells, $pp60^{c\text{-}src}$ distributes, in part, uniformly over the cell surface and, in addition, there occurs a typical clustering of $pp60^{c\text{-}src}$ containing patches in the region of the centrosomes of interphase cells. At the G2-to-M-phase transition, the distribution patterns of $pp60^{c\text{-}src}$ drastically change to become essentially diffuse and patchy throughout mitosis. The preferential $pp60^{c\text{-}src}$ aggregation in the region of the centrosomes and the uniformly dispersed distribution at the level of the cell surface do not develop again until late telophase.

The observation of the immunolocalization patterns of $pp60^{c\text{-}src}$ in the NIH c-*src* overexpresser cells during interphase and at different phases during mitosis led us to advance the hypothesis that $pp60^{c\text{-}src}$ may be associated with endocytotic vesicles. The induction of patching and capping of cell surface molecules by labeled lectins in a variety of cells, followed or not by endocytosis of the lectin–receptor complexes, is the model system that has been the most extensively used to examine the possible mechanism of initiation and processing of endocytosis (Ash and Singer, 1976; Albertini and Anderson, 1977). The second part of this article describes experiments in which the NIH (pM c-*src*/focus) B cells and control NIH 3T3 cells were exposed, for various times to unlabeled or fluorescently labeled Con A and the fate of the labeled lectin was compared with that of

$pp60^{c\text{-}src}$. In both cells, after 15 min of incubation, the fluorescent lectin was found to condense at the level of the cell surface into patches that coincided with $pp60^{c\text{-}src}$-containing patches in the NIH c-src overexpresser cells. After a longer incubation time, aggregation of the fluorescent patches was found to occur near the cell center in a juxtanuclear position in both cells. The intracellular Con A caps also stained for $pp60^{c\text{-}src}$ in the c-src overexpresser mouse cells. These observations suggest that $pp60^{c\text{-}src}$ might participate in the patching, endocytosis and capping of Con A–receptor complexes in the NIH (pM c-*src*/focus)B cells.

Materials and Methods

Cells and Immunochemical and Staining Reagents

NIH 3T3 cells and NIH (pMc-*src*/focus)B cells were kindly provided by D. Shalloway (Cornell University) (Shalloway et al., 1984) and were cultured on 22-mm² coverslips in DME containing 5% (vol/vol) newborn calf serum and antibiotics under an atmosphere of 10% CO_2/air for at least 2 d at 37°C before the labeling experiments. The average cell density was 2.10^3 cells per cm². When cultures enriched in premitotic and mitotic cells were to be examined, plating of the cells was effected at a higher density ($\sim 5.10^3$ cells per cm²) and the medium was changed the evening preceding the experiment to stimulate mitosis.

The antibody used to detect $pp60^{c\text{-}src}$ was the mouse monoclonal antibody, mAb 327, initially obtained by Lipsich et al. (1983) and commercialized by Cliniosciences (Paris, France). Double-immunofluorescence labeling for $pp60^{c\text{-}src}$ and tubulin was performed using mAb 327 and a rat monoclonal anti-tubulin (Biosys). Secondary antibodies were Fab fragments from sheep IgG against mouse IgG conjugated either with FITC (Biosys, Compiègne, France) or with tetramethyl rhodamine isothiocyanate (TRITC; Biosys) and goat IgG against rat IgG adsorbed on columns of mouse IgG and conjugated with the same chromophores as the anti–mouse IgG. These secondary antibodies were giving a quasi-undetectable background fluorescence. In mitotic cells, labeling for $pp60^{c\text{-}src}$ and tubulin was observed independently. Indeed, tubulin staining in these cells is so strong that leakage of the tubulin-associated fluorescence is very often observed at the wave length at which the $pp60^{c\text{-}src}$-associated fluorescence is observed. Evidence that the cells labeled for $pp60^{c\text{-}src}$ and those labeled for tubulin were in the same mitotic phase was provided by observation of the chromosome arrangement by phase contrast microscopy (Berlin et al., 1978). The actin containing structures were visualized using nitrobenzoxadiazole (NBD)-phallacidin (Molecular Probes, Inc., Beaverton, OR; Barak et al., 1980).

TRITC-conjugated Con A and FITC-conjugated wheat germ agglutinin were used as markers, for the rough reticulum endoplasmic and for the Golgi apparatus respectively (Vector Laboratories, Inc., Burlingame, CA; Virtanen et al., 1980).

Fluorescence Studies and Microscopy

Simple or double fluorescent labeling of the cells was carried out as described earlier (David-Pfeuty and Singer, 1980) after fixation with 3% formaldehyde and permeabilization by treatment with 0.1% Triton X-100 at room temperature. Control experiments were performed on NIH 3T3 cells that express a level of $pp60^{c\text{-}src}$ too low to be detectable by the immunofluorescence technique.

The labeling of the ConA receptors was effected following the procedure of Ash and Singer (1976). The coverslips maintained in 35-mm dishes on which cultured cells were grown, rinsed three to four times with serum-free DME, and incubated with 1 ml of the same medium containing 50 μg of either unlabeled ConA or F-ConA for various times at 37°C. After being rinsed three to four times again, they were fixed with 3% formaldehyde in PBS at room temperature and either they were observed at that time or they were processed as described above for fluorescent labeling of intracellular components after permeabilization by treatment with 0.1% Triton X-100.

Fluorescent microscopy was performed with a Leitz microscope equipped with filter settings for fluorescein and rhodamine. The microscope was also equipped for phase contrast, which allowed the identification of the mitotic cells and of the mitotic phases through the examination of the chromosome arrangement and following the criteria given by Berlin et al.

(1978). The observations were made either with a X40 or X63 oil objective. Photographs were taken on a Kodak T-Max 400 film.

In double-fluorescent labeling experiments, we used reagents each coupled separately FITC and to TRITC and we examined the two possible combinations.

Results

Localization Patterns of pp60^{c-src} in Interphase NIH (pM c-src/focus)B Cells

The c-src overexpresser cells, NIH (pM c-src/focus)B, have been reported to exhibit morphology characteristics intermediate between those of normal NIH 3T3 cells and v-src-transformed cells, on the ground that they are more rounded and refractile than the NIH 3T3 cells, although not as much as the v-src-transformed cells (Shalloway et al., 1984). Our data are in agreement with this observation mainly when the cells are examined near confluency. However, when the cells are plated at low or medium density, the morphological aspect of the c-src overexpresser cells resembles closely that of the normal NIH 3T3 cells. Both cell types do not spread very well on glass or plastic and they have a propensity to develop long cellular processes, possibly more so for the NIH (pM c-src/focus)B cells.

When the cells are immunolabeled with mAb 327 that recognizes specifically both pp60^{v-src} and pp60^{c-src}, a weak, unspecific, and diffuse staining is observed in the control NIH 3T3 cells that concentrates in the central region of the cells over and around the nucleus (Fig. 1 A). The NIH (pMc-src/focus)B cells express ~20 times more chicken pp60^{c-src} than endogeneous pp60^{c-src}. Their immunolabeling with mAB 327 reveals several characteristic features of the pp60^{c-src} localization. A first and constant feature is the appearance of a uniformly dispersed fluorescence covering the inner side of the cell surface with no clearly discernible structure (wide arrow, Fig. 1 b). Besides this plasma membrane-associated staining, a bright spot is apparent in many cells that locates over the cell nucleus or in tight contact with the nuclear envelope (thin arrows, Figs. 1, b and d, 3, a and b). In some instances, it could be noticed that label was absent from the middle of this bright spot (thin black arrows, Fig. 3 b). Also, one observes a more or less dense clustering of fluorescent patches, somewhat smaller than the nucleus-associated spot, surrounding the periphery of the nucleus either partially or totally (wide arrowheads, Fig. 1, b, d, h, and i). This perinuclear staining spreads away from the nucleus towards the cell periphery to an extent which varies from one cell to another. Often, but not always, the long cellular processes developed by the NIH (pM c-src/focus)B cells plated at low density are heavily stained (Fig. 1 g). When the tip of one such process meets a neighboring cell, lamella formation and spreading over this neighbor occurs (arrowhead, Fig. 1 c). It seems, therefore, that the NIH (pM c-src/focus)B cells spread much better on other cells than on a glass or plastic substratum. This deficiency in spreading capacity is responsible for the appearance of the long cellular processes, whose formation is inhibited when the c-src overexpresser cells are plated at high density or when they are plated at low density on a confluent layer of irradiated NIH 3T3 cells (Fig. 1 i). Finally, as in the c-src

overexpresser MDCK cells (Warren et al., 1988), pp60^{c-src} also accumulates at cell–cell contact areas, either in a diffuse way (thin white arrows, Fig. 1 h) or in small strikes that are also enriched in actin where the leading lamellas of two neighboring cells meet (thin white arrows, Figs. 1, e and f and 3 a). Such contacts, however, are not frequently encountered, even in nearly confluent cultures, since the margin of one cell will tend to spread out over the upper surface of the neighboring cell (thick arrows, Fig. 3 a), as was noticed earlier for the tips of the cellular processes.

Comparison between the Localization Patterns of pp60^{c-src} and of Intracellular Structures

We next compared the intracellular distributions of pp60^{c-src} in the NIH (pM c-src/focus)B cells and of two labeled lectins, FITC-wheat germ agglutinin and TRITC-Con A, that preferentially label respectively the Golgi apparatus and the rough (R) ER (Virtanen et al., 1980). The three exhibit a perinuclear location, so it is not surprising that they appear to partially colocalize. However, the Golgi apparatus generally concentrates in a narrow space close to the nuclear envelope and the cluster of pp60^{c-src}-containing patches almost always extends further away from the nucleus than the Golgi apparatus (Fig. 2, c and d). The reverse is true with the RER, which always tends to invade the cellular cytoplasm further away from the nucleus than the cluster of pp60^{c-src} containing patches (Fig. 2, a and b). The three patterns, therefore, do not seem to coincide, although partial overlap occurs.

Double immunolabeling experiments with mAb 327 and a rat anti-tubulin mAb were also performed. These experiments clearly indicate that the location of the central, pp60^{c-src}-containing spot over the nucleus coincides exactly with the centriolar region in which converge the interphase microtubules. Moveover, the cluster of pp60^{c-src}-containing patches that surrounds the nucleus appears to be embedded inside a dense meshwork of microtubules (compare Fig. 3, a–c to 3, a'–c'). Apparently, there was a correlation between the degree of accumulation of pp60^{c-src}-containing patches in the region of the centrosomes and the density of the microtubule meshwork in the same region. The area of the cell containing the centriole is known to play the role of microtubule organizing center (MTOC), so we examined the effect of microtubule disruption on the distribution of pp60^{c-src}. The incubation of the cells in the presence of 10 μg/ml nocodazole for 90 min results in a scattering of the pp60^{c-src}-containing patches throughout the cytoplasm and disappearance of the nucleus-associated fluorescent spot (Fig. 2 g). Therefore, the clustering of the pp60^{c-src}-containing patches in the region of the MTOC depends on the presence of microtubules and pp60^{c-src} is not associated directly with the centriole. The latter conclusion is consistent with the observation reported in the previous section that, in some instances, labeling for pp60^{c-src} appears to be excluded from the center of the nucleus-associated fluorescent spot. Upon treatment with nocodazole or other microtubule disrupting agents, the Golgi elements and the RER as well, disseminate through the cytoplasm (Louvard et al., 1982). The RER and Golgi vesicles generated under these conditions did not coincide with the scattered pp60^{c-src}-containing patches (not shown).
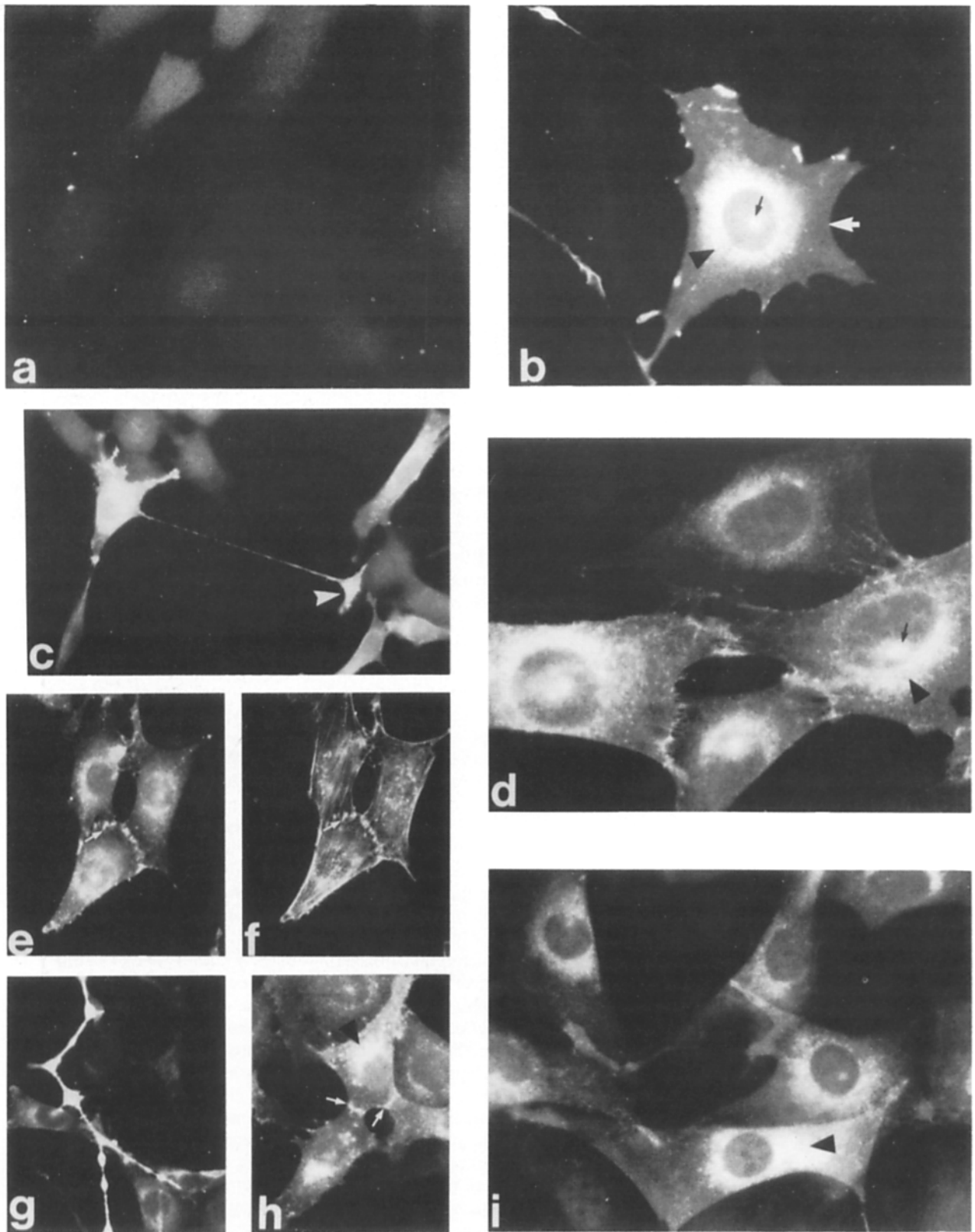
Figure 1. The NIH 3T3 (*a*) and the NIH (pM c-*src*/focus)B cells (*b–i*) were immunolabeled with mAb 327 (except *f*, in which actin labeling was performed with NBD-phallacidin) followed by FITC or TRITC-Fab fragments from sheep IgG to mouse IgG. The following features are pointed out: the compact juxtanuclear pp60$^{c\text{-}src}$-containing spot (*thin black arrows* in *b* and *d*); the perinuclear clustering of pp60$^{c\text{-}src}$-containing patches (*black arrowheads* in *b, d,* and *i*); the uniform plasma membrane-associated fluorescence (*thick white arrow* in *b*); the lamella formation and spreading of the tip of a long cellular process over a neighboring cell (*white arrowhead* in *c*); the pp60$^{c\text{-}src}$ accumulation in association with actin in cell-to-cell contact areas (*thin white arrows* in *e, f,* and *h*); a long neurite-like process that is heavily stained (*g*). *a, b,* and *i,* ×500; *c, e–h,* ×250; *d,* ×700.
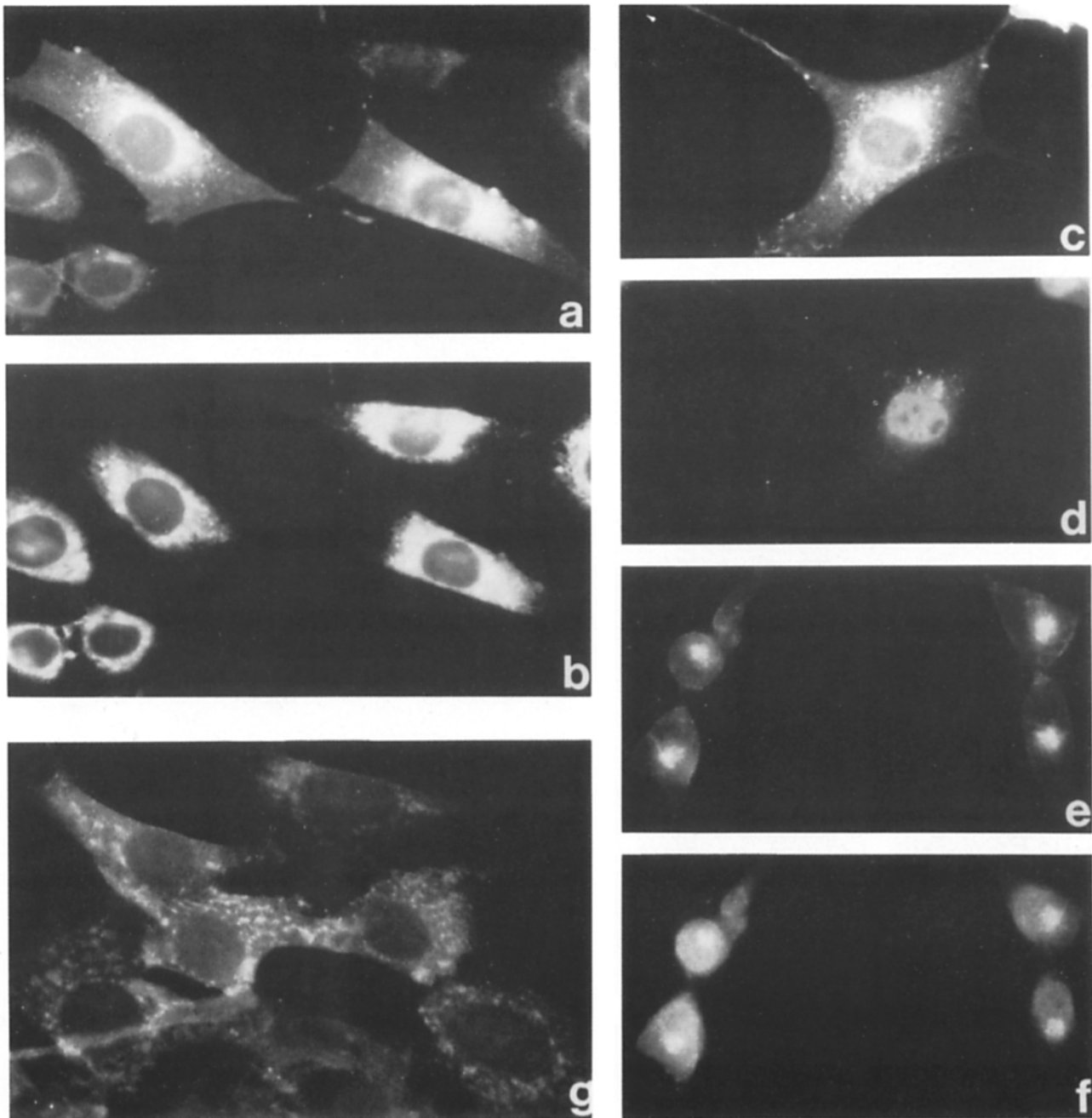
Figure 2. The NIH (pM c-*src*/focus)B cells were stained for pp60$^{c\text{-}src}$ (*a, c, e,* and *g*) as described in the previous figure and simultaneously with the fluorescently labeled lectins TRITC-Con A (*b*) or FITC-WGA (*d* and *f*). In *g*, pp60$^{c\text{-}src}$-staining was performed after treatment with 10 μg/ml nocodazole for 90 min. *a–d, g,* ×500; *e* and *f,* ×250.

Localization of pp60$^{c\text{-}src}$ during Premitotic Phase and Mitosis

During the premitotic (G2) phase that occurs between the phase (S) of DNA synthesis and the onset of mitosis, the two centriole pairs (diplosomes) separate from one another. The NIH (pM c-*src*/focus)B cells in G2 phase are easily recognized after double immunofluorescent labeling for pp60$^{c\text{-}src}$ and tubulin: two nucleus-associated foci from which microtubules radiate in all directions are decorated with mAb 327 (Fig. 3, *b* and *b'*; Fig. 4, *a, b* and *b'*). Microtubules directing away from the opposite centriole pair form a set of

astral rays (*thick white arrow,* Fig. 3 *b'*) and those pointing toward the opposite centriole pair will become components of the continuous mitotic spindle (McIntosh et al., 1969) (*thick black arrow,* Fig. 3 *b'*). During that stage, the cell starts shrinking, the astral microtubules shorten and the perinuclear labeling with mAb 327 appears to condense around the two diplosomes when these reach a symmetrical location within two nuclear invaginations (Fig. 4, *c–e*). At the end of that stage, often, the plasma membrane-associated pp60$^{c\text{-}src}$ fluorescence becomes more intense and looks rather patchy (Fig. 4 *d*). At the same time, part of the pp60$^{c\text{-}src}$ staining shows a high degree of agglutination around
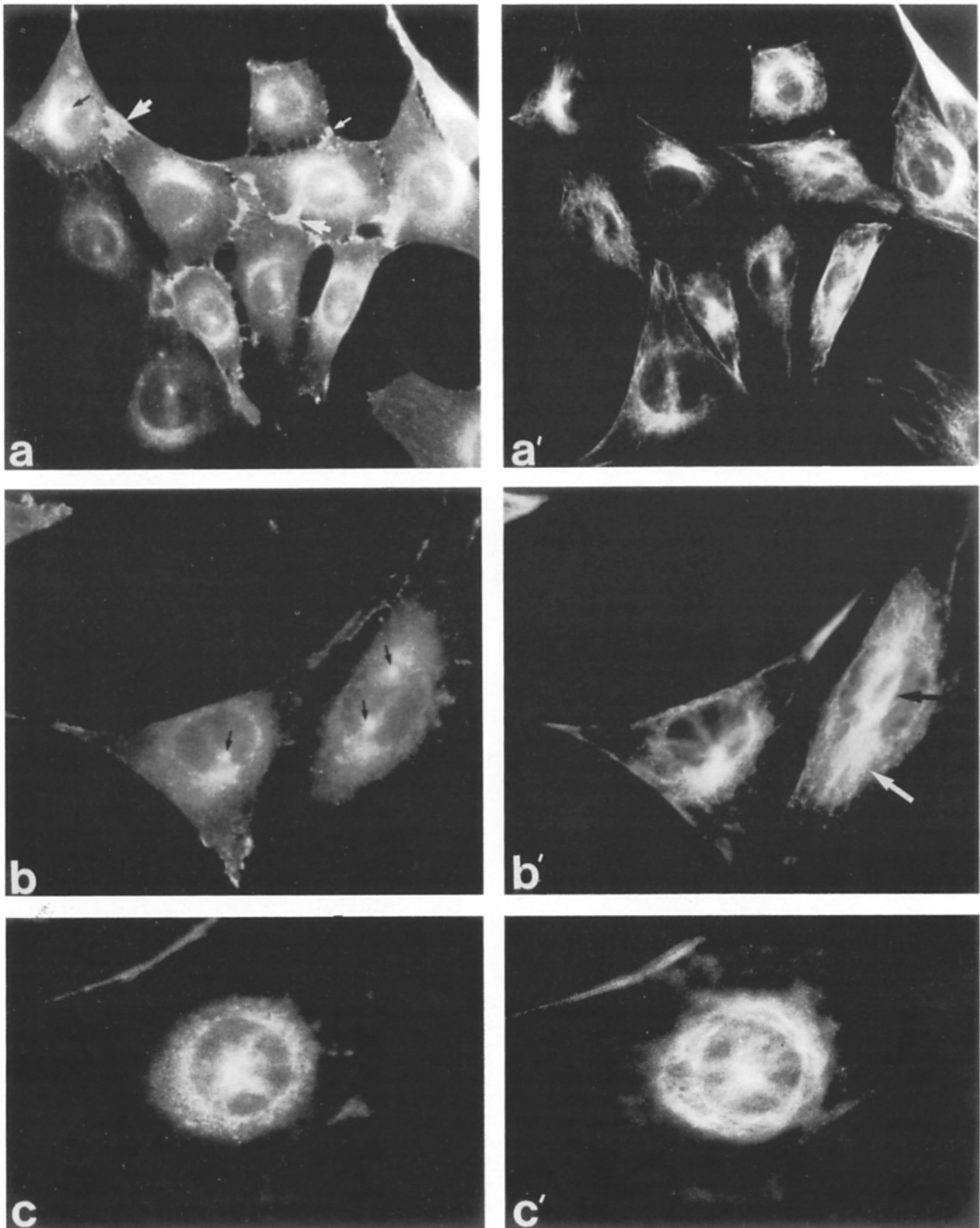
Figure 3. The NIH (pM c-*src*/focus)B cells were stained for pp60^{c-src} (*a–c*) as described in the previous figures and simultaneously for tubulin (*a′–c′*) with monoclonal rat anti-tubulin followed by goat TRITC-IgG to rat IgG. The following features are pointed out: the compact juxtanuclear pp60^{c-src}-containing spot (*thin black arrows* in *a* and *b*) that coincides with the centriolar region (compare *a* and *b* and *a′* and *b′*); in *b*, label appears to be excluded from the middle of the fluorescent spots; the lamella spreading between neighboring cells (*thick white arrows* in *a*); a set of astral microtubules (*thick white arrow* in *b′*); a set of microtubules interconnecting the diplosomes (*thick black arrow* in *b′*); the perinuclear cluster of pp60^{c-src}-containing patches is best visualized together with a perinuclear meshwork of microtubules when the focus is at the mid-level of the cell (*c* and *c′*). *a* and *a′*, ×400; *b* and *b′*, ×700; *c* and *c′*, ×800.

the two diplosomes and another diffuse part breaks through the cytoplasm (Fig. 4 *d*). The degree of diffuse fluorescence may vary from one cell to another, but the pericentriolar staining is always observed.

The various phases of mitosis can be followed by examining the arrangement of the chromosomes using phase-contrast microscopy (Berlin et al., 1978). Prophase begins with the earliest detectable chromosome condensation after the breakdown of the nuclear envelope. During that phase (Fig. 4, *f* and *g*), the distribution pattern of pp60^{c-src} keeps changing: the two pericentriolar pp60^{c-src} clusters become less compact and less prominent and the intracellular pp60^{c-src} staining is now essentially patchy and diffuse, whereas the surface fluorescence proportionally decreases. At this stage the aster microtubules have almost totally depolymerized. The apparent dissolution of the pericentriolar pp60^{c-src} clusters intensifies during prometaphase when the chromosomes start lining up along the metaphase plate and when the fluorescence staining for tubulin becomes more spindle shaped (Brinkley et al., 1975; Fig. 4, *h* and *i*). In metaphase (Fig. 4, *j–n*), cells may or may not exhibit a residual pericentriolar pp60^{c-src} fluorescence and they continue to exhibit the intracellular diffuse and patchy pp60^{c-src} fluorescence. During these phases, a faint fibrillar pp60^{c-src} staining that emanates from the spindle poles can be sometimes observed (*arrow*, Fig. 4 *m*). In anaphase (Fig. 4, *o–q*), and in early telophase, generally, the intracellular diffuse pp60^{c-src} fluorescence predominates, whereas a patchy pp60^{c-src} fluorescence is observed when the microscope is focused at the level of the cell surface (either upper or at the cell–substrate interface). This patchy surface fluorescence, which is finely punctuated, is clearly distinct from the intracellular one observed between prophase and metaphase.

A new striking change occurs in late telophase. At the same time as a slight peripheral pp60^{c-src} fluorescence, a dense and diffuse pp60^{c-src} staining appears at the interface between the daughter-forming cells, except at the level of the midbody (Fig. 4 *r*). Also, pp60^{c-src} starts to concentrate again, together with the Golgi apparatus, in the MTOC regions of the two daughter cells (Fig. 2, *e* and *f*; Fig. 4 *r*). As the daughter cells separate further, pp60^{c-src} does not remain concentrated in the region between the daughter cells, which now are connected through the cleavage furrow and the midbody (Fig. 4 *s*). Rather, a finely punctuated surface fluorescence redistributes, becoming more homogeneous and intense, whereas the diffuse cytoplasmic staining decreases proportionally (Fig. 4, *t* and *u*), until it eventually vanishes as the two daughter cells further spread on the substratum. The characteristic pp60^{c-src} distribution patterns of interphase cells are generally recovered before the two daughter cells part company (Fig. 4 *w*).

Con A Patterns in Normal and c-src Overexpresser NIH 3T3 Cells

The distribution of fluorescently labeled Con A was examined at three different times (0, 15 min, 1 h) after the exposure of the cells to the fluorescent lectin at 37°C. Whether normal or c-*src* overexpresser NIH 3T3 cells were used, the Con A patterns were identical.

Initially, the fluorescence covered the cell surface uniformly with no discernible structure, in accordance with the

earlier report of Ash and Singer (1976, Fig. 5 *a*). Also, initially as well as after various incubation times, an accumulation of F-Con A was observed external to the cells, as packs or as a meshwork of imbricated linear filaments (*arrowheads*, Fig. 5 *a*). This latter labeling was due to the binding of F-Con A to the fibronectin component of the extracellular matrix, which is known to be a Con A receptor (Burridge et al., 1976; our own observations). The intracellular actin skeleton visualized with NBD-phallacidin did not differ significantly between the untreated normal and c-*src* overexpresser NIH 3T3 cells (Fig. 6, *b* and *d*). In general, the actin cables are not very well developed, mainly in cells that are not well spread or exhibit an elongated shape. Some membrane ruffling may also be observed (*arrowheads*, Fig. 6 *d*).

After 15 min of incubation in the presence of F-Con A, the gross morphology of the treated cells appeared unchanged. If, however, the intracellular actin skeleton was stained, an extensive membrane ruffling was observed at the cell periphery (*arrowheads*, Fig. 6, *f* and *g*) and the actin cables no longer appeared as continuous, linear structures, like in many untreated cells but rather, they appeared as dotted linear arrays (Fig. 6, *f* and *g*). Here, the fluorescent Con A was redistributed into bright punctuated patches (or dots) which arranged in part into linear arrays, visible at the cell surface level in different regions of the cells (Fig. 5, *b–f* and Fig. 6 *h*), particularly in pseudopods (*thin arrows*, Fig. 5 *e*), at the cell–substratum interface, most often below the nucleus (Fig. 5, *b* and *d* and Fig. 6 *h*) and at the upper cell surface, above the nucleus (Fig. 5*f*). Another part concentrated around the nucleus in a cluster of patches that were somewhat bigger than the plasma membrane-associated ones (*arrowheads*, Fig. 5, *c* and *e*).

After 1 h of exposure to the F-Con A, many cells (>60%) had shrunk. In these smaller and more rounded cells, the well-defined plasma membrane-associated dots had almost totally vanished from the cell surface. Instead, most of the fluorescent lectin now concentrated into a rather large aggregate (or cap) situated near the cell center, adjacent to the nucleus (Fig. 5, *g* and *h*). This aggregate was apparently made up of a number of fluorescent patches that could be distinguished, in part, when the focus was set at the mid level of the cell (Fig. 5 *g*) and, for the other part, at the cell–substratum interface (Fig. 5 *h*).

pp60^{c-src} Patterns in Con A-treated c-src Overexpresser NIH 3T3 Cells

The NIH (pM c-*src*/focus)B cells were exposed to unlabeled Con A at 37°C for different times, after which they were washed, fixed, and permeabilized before labeling with the mAb 327. When the pp60^{c-src} staining of the cells was carried out after a short exposure time to the lectin (<30 s), the majority of the interphase mouse cells exhibited the characteristic pp60^{c-src} patterns previously described for untreated cells (first section, Fig. 7 *a*).

The uniform plasma membrane-associated pp60^{c-src} fluorescence generally persisted in the cells that had been exposed to Con A for 15 min. However, in addition, a punctuated pp60^{c-src} fluorescence was breaking through at the inner cell surface level, mainly, in pseudopods (Fig. 7 *c*), at the cell substratum interface, below the nucleus (Fig. 7, *b* and *d*), and above the nucleus (Fig. 8 *g*). Also, a cluster of
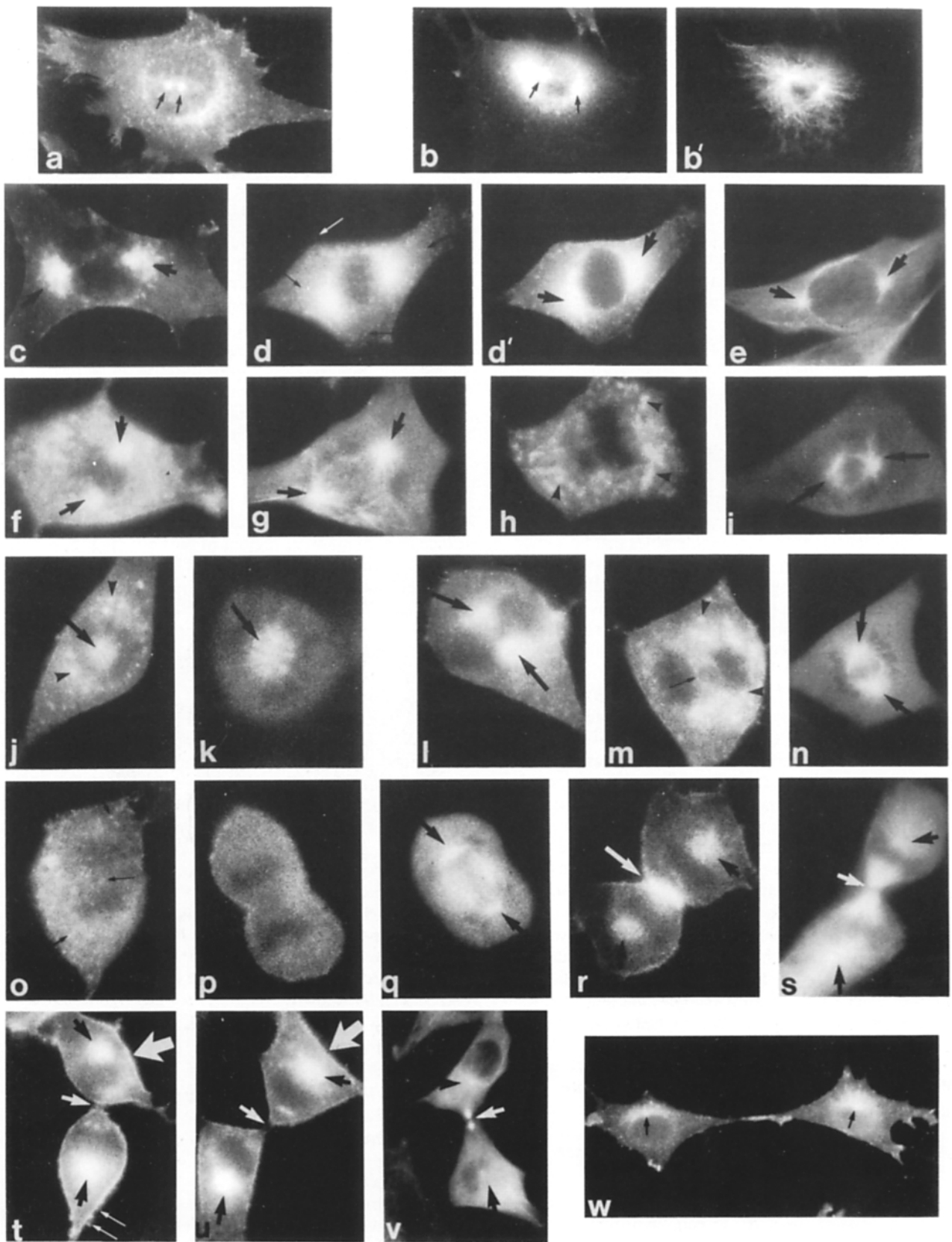
Figure 4. Immunolabeling of pre-mitotic and mitotic NIH (pM c-*src*/focus)B cells for pp60^c-src and tubulin. First row, in G2 phase, the two centriole-pairs that stains for pp60^c-src (*thin arrows, a* and *b*) and from which irradiate microtubules (*b'*), separate. Second row, late G2, pp60^c-src agglutinates around the centriole pairs (*black arrow* in *c* and *d'*); interphase microtubules have already depolymerized (*e*), a finely punctuated pp60^c-src fluorescence is present at the cell surface (*thin arrows* in *d*). In prophase (*f* and *g*), prometaphase (*h* and *i*) and metaphase (full face view in *j* and *k*; transversal view in *l–n*), four pp60^c-src locations are observed: diffuse, intracellular patchy (*ar-*

perinuclear $pp60^{c-src}$-containing patches was observed, as in untreated cells (Fig. 7 e), but, most often, the compact centriolar spot inside the juxtanuclear region of fluorescence either had vanished or was replaced by a loose cluster of small patches (arrowheads, Fig. 7 b).

Treatment of the cells for 1 h with the lectin resulted in the redistribution of the $pp60^{c-src}$ fluorescence into two pools: a diffuse one spreading uniformly through the cytoplasm (black arrow, Fig. 7 f) and a patchy one that agglutinated into a juxtanuclear aggregate (wide white arrow, Fig. 7 f), a part of which appeared to lie at the bottom of the cells, at the cell–substratum interface (wide open arrow, Fig. 7 g). In some instances, this latter part of fluorescence was absent and instead, clusters made up of a few (two to four) $pp60^{c-src}$-containing dots were located at the lower cell surface level (Fig. 6 h). When the cells were double-stained for $pp60^{c-src}$ and actin, actin-containing aggregates were often seen in association with that part of the aggregate lying at the bottom of the cell (arrows, Fig. 6, k and l), but not with the inner part of it (Fig. 6, i and j). Moreover, actin bundles were no longer present.

Simultaneous Observation of the $pp60^{c-src}$ and Con A Patterns in NIH c-src Overexpresser Cells

The same study as that described in the previous section was undertaken, but, using fluorescent, instead of unlabeled Con A, to visualize the $pp60^{c-src}$ and Con A patterns on the same cell.

Initially, both a part of the $pp60^{c-src}$ labeling and that of F-Con A is found uniformly dispersed at the cell surface level (on the external face for F-Con A, on the cytoplasmic face for $pp60^{c-src}$). No F-Con A is present inside the cells at a location similar to that of the centrosomal $pp60^{c-src}$ population (Fig. 8, a and b).

On cells exposed to F-Con A for 15 min, patching of F-Con A and of $pp60^{c-src}$ occurs at the cell surface level as described in the two previous sections. When the F-Con A and $pp60^{c-src}$ labelings are observed on the same cell, it is clear that the plasma membrane-associated patches labeled with F-Con A and those containing $pp60^{c-src}$ do superimpose (compare Fig. 8, c, e, g, and i and d, f, h, and j). An evident coincidence also exists between the clustered, perinuclear patches labeled with F-Con A and those labeled by the mAb 327 (wide white arrows; Fig. 8, i and j). Two main differences, however, can be noted between the overall $pp60^{c-src}$ and Con A patterns: (a) a uniformly dispersed plasma membrane-associated $pp60^{c-src}$ fluorescence still remains, although not as intense as in the untreated cells, whereas the initially uniform plasma membrane-associated Con A fluorescence has, in many cases, almost totally vanished; (b) when

a residual centriolar $pp60^{c-src}$ spot of fluorescence is still present, F-Con A is absent from that $pp60^{c-src}$ location (black arrows, compare Fig. 8, c and i and d and j).

Upon 1 h of exposure to F-Con A, large juxtanuclear aggregates containing the fluorescent lectin and $pp60^{c-src}$ have formed in >60% of the cells. Here again, the striking similarity observed between the architecture of the caps labeled respectively with F-Con A and for $pp60^{c-src}$, strongly suggests that the two caps are a single entity to which both components are associated (compare Fig. 8 k with l and Fig. 9, a, c, and e, and b, d, and f). A few additional features of the overall $pp60^{c-src}$ and Con A patterns can also be pointed out: (a) the F-Con A is not found, contrary to $pp60^{c-src}$ diffusely located in the cytoplasm (compare Fig. 9, a, c, and e with b, d, and f); (b) the appearance of a diffuse cytoplasmic $pp60^{c-src}$ fluorescence seems to occur concomitant with the disappearance of the $pp60^{c-src}$ labeling at the plasma membrane level; (c) occasionally, a higher concentration of $pp60^{c-src}$ and/or of F-Con A may be found associated with the plasma membrane in sparse regions of the cell (arrowheads, Fig. 9, a and b); (d) a location of $pp60^{c-src}$ in a compact centriolar spot inside the juxtanuclear region of fluorescence is very often observed after 1 h of exposure of the cells to F-Con A. However, when the F-Con A staining is not too intense, one can notice that F-Con A is never present at this site in association with $pp60^{c-src}$ (thin white arrows, Fig. 9, e and f); (e) if the cells treated with F-Con A for 1 h are stained in parallel with fluorescent wheat germ agglutinin, which reveals the Golgi apparatus (Virtanen et al., 1980), one observes a coincidence between the F-Con A cap and that intracellular structure (arrows, Fig. 9, q and r).

When the double-labeling experiments described above are performed on the control NIH 3T3 cells that express ~20 times less $pp60^{c-src}$ than the NIH (pM c-src/focus)B cells, the F-Con A patches and aggregates that form in this system are not detectably labeled with the mAb 327 (not shown).

$pp60^{c-src}$ and Con A Patterns in Mitotic c-src Overexpresser Cells

At the G2-M phase transition, a striking redistribution of $pp60^{c-src}$ has been shown to take place. In particular, in late G2 phase, the plasma membrane fluorescence becomes patchy, a diffuse cytoplasmic $pp60^{c-src}$ fluorescence breaks through, and a strong agglutination of $pp60^{c-src}$-containing patches occurs around the two diplosomes. After exposure to F-Con A for 15 min, one observes, during this premitotic phase, an agglutination of F-Con A patches around the diplosomes, in structures that superimpose on the two diplosomal $pp60^{c-src}$-containing clusters (Fig. 9, g–j). From prophase to anaphase, the two prominent distributions of $pp60^{c-src}$ are

---

rowheads in h, j, and m), residual pericentriolar (arrows in f, j, and l) and fibrillar (thin arrows in m); the black arrows indicate in g, a residual pericentriolar tubulin staining and in i, k, and n the spindle poles labeled with anti-tubulin antibodies. In anaphase (o–q), the spindle poles move apart (arrows in q) and $pp60^{c-src}$ is found either diffusely distributed inside the cell (p) or finely punctuated on both cell surfaces (o: top). In early telophase, a strong fluorescence appears at the interface between the daughter forming cells (white arrow in r). The speckled $pp60^{c-src}$ cell surface fluorescence is still present (thin arrows in t) and a juxtanuclear $pp60^{c-src}$ cluster reappears (black arrows in r, t, and u) that coincide with the MTOC (black arrows in s and v). $pp60^{c-src}$ is excluded from the midbody region (white arrows in s–v). The daughter cells, often, recover the characteristic $pp60^{c-src}$ patterns of interphase cells before their full separation (w). a–u, ×600; v and w, ×250.
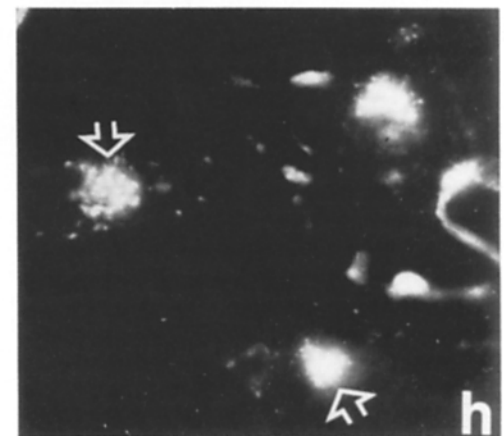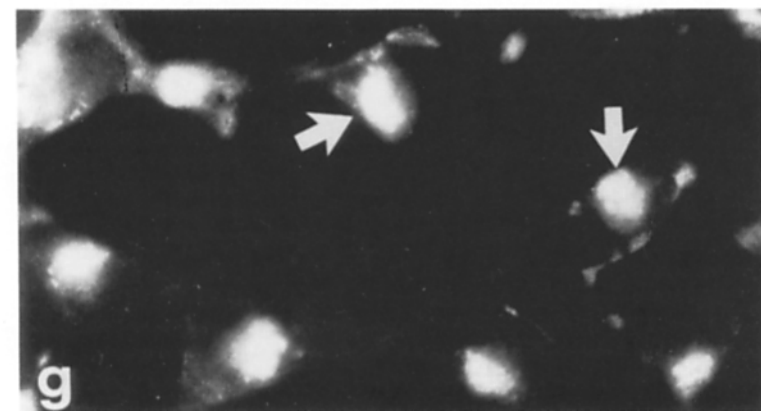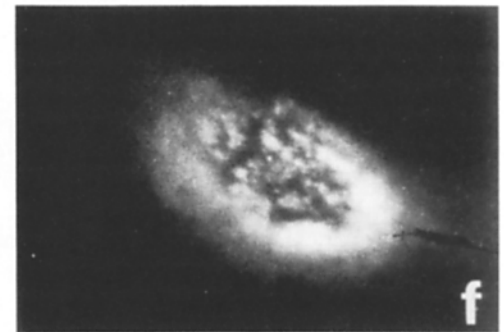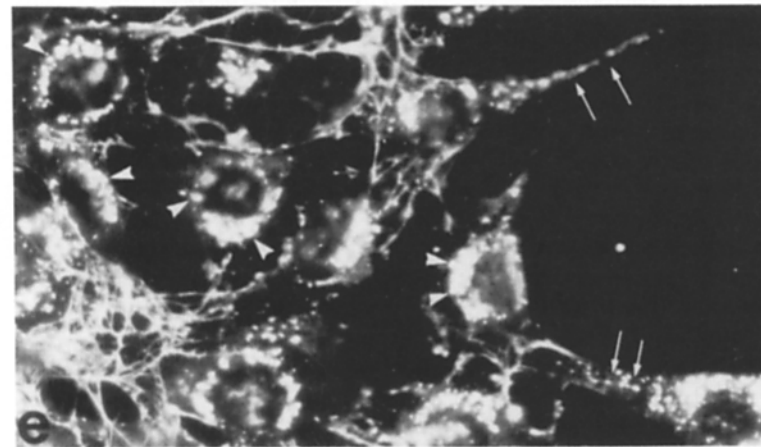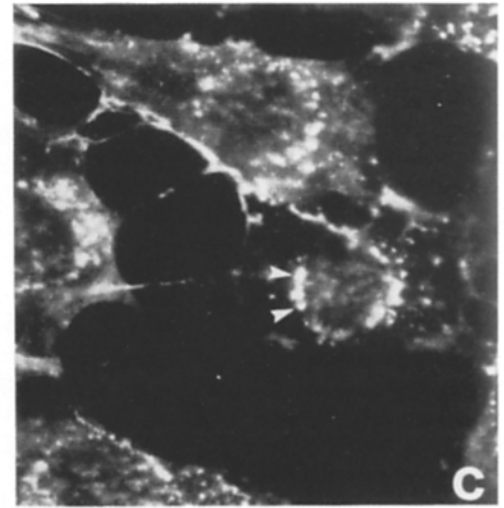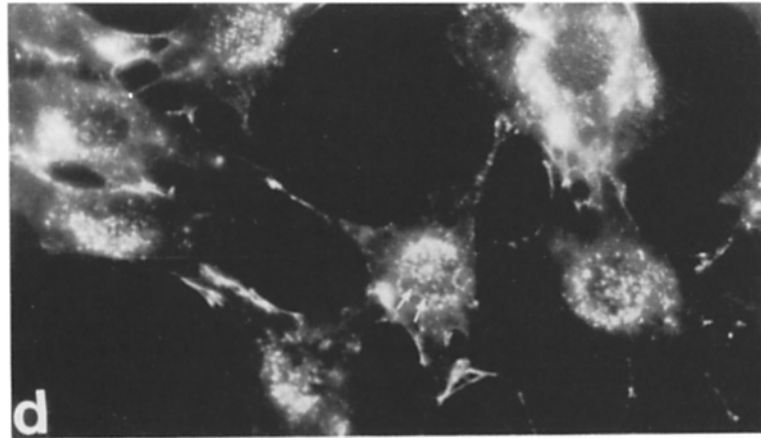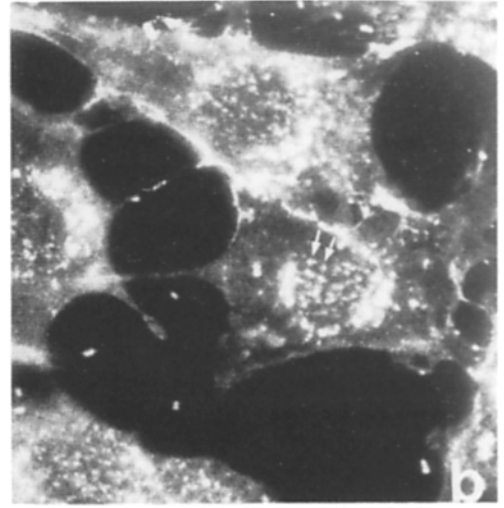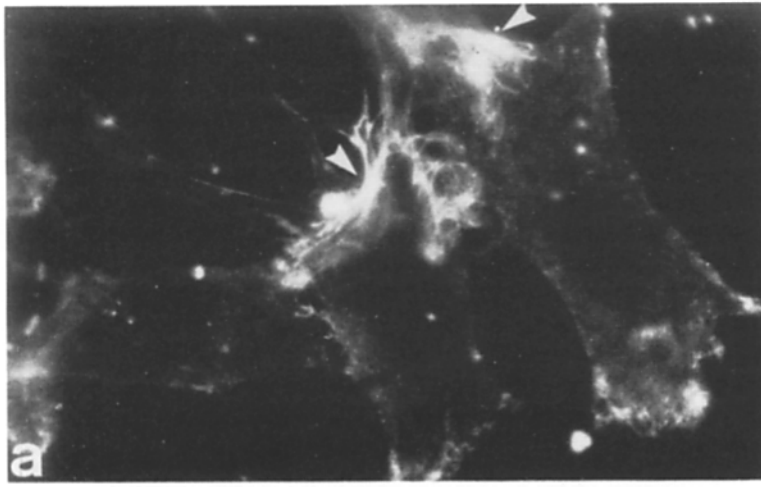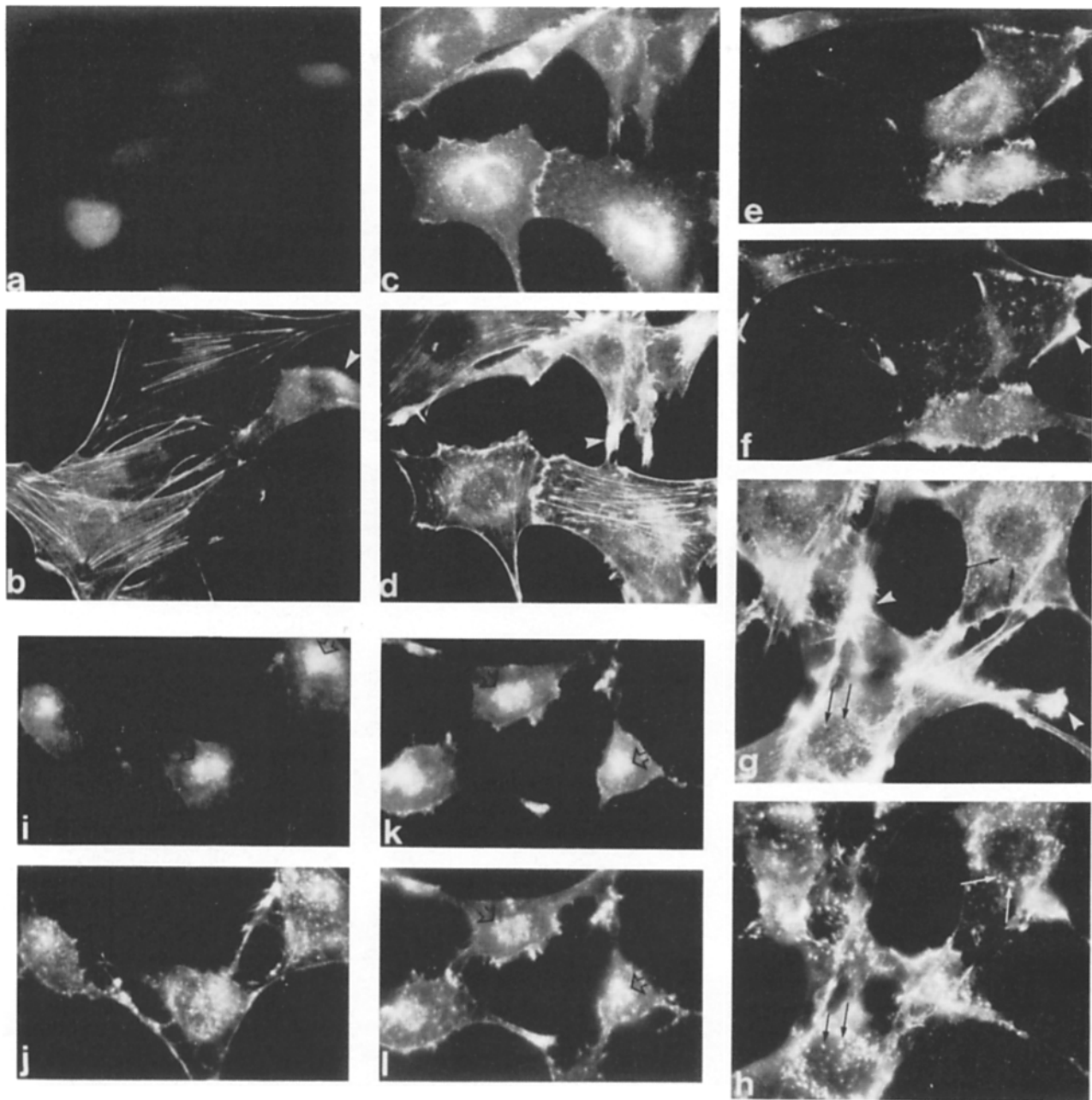
Figure 6. Simultaneous visualization of actin skeletons (*b, d, f, g, i,* and *k*) and mAb 327 staining (*a, c, e, i,* and *k*) on the same cells or F-Con A staining (*h*). The NIH 3T3 (*a* and *b*) and the NIH (pM c-*src*/focus)B cells (*c–l*). (*a–d*) Untreated cells; (*e–h*) cells treated with ConA for 15 min and for (*i–l*) 1 h. A limited ruffling activity is observed in untreated cells, an extensive one in Con A-treated cells (*arrowheads* in *b, d, f,* and *g*). After 15 min incubation with Con A, the actin arrangement becomes essentially linearly punctuated. Actin patches appear to coincide sometimes with F-Con A patches (*arrows* in *g* and *h*). After 1 h of incubation, actin cables have totally vanished. Actin appears associated with that part of the Con A- and pp60^{c-src}-containing cap standing at the bottom of the cell (*open arrows* in *k* and *l*) but not with the intracellular part. *i* and *j,* ×300.

Figure 5. Fluorescence patterns of F-Con A after exposure of NIH (pM c-*src*/focus)B cells to the lectin for various times. The focus was set at the bottom in *a, b, d,* and *h*; at the mid level of the cells in *c, e,* and *g*; at the upper cell surface level in *f.* After 15 min of exposure to F-Con A the initially uniform, plasma membrane-associated Con A fluorescence (*a*) was redistributed in different structures: (*a*) in tiny dots that are frequently observed linearly arranged at the cell bottom (*short arrows* in *b* and *d*); (*c*) in dots that are located at the upper cell surface level (*f* and *long arrows* in *e*); (*c*) in globular aggregates bigger than the previously described dots, that cluster around the nucleus (*arrowheads* in *c* and *e*). After 1 h of exposure to F-Con A, one observes an aggregation of F-Con A patches into a large cap that stands near the cell center in a juxtanuclear position (*wide arrows* in *g*), a part of which remains apparently associated with the lower cell surface (*open arrows* in *h*). *a–c, g, h,* ×500; *d* and *e,* ×300; *f,* ×700.
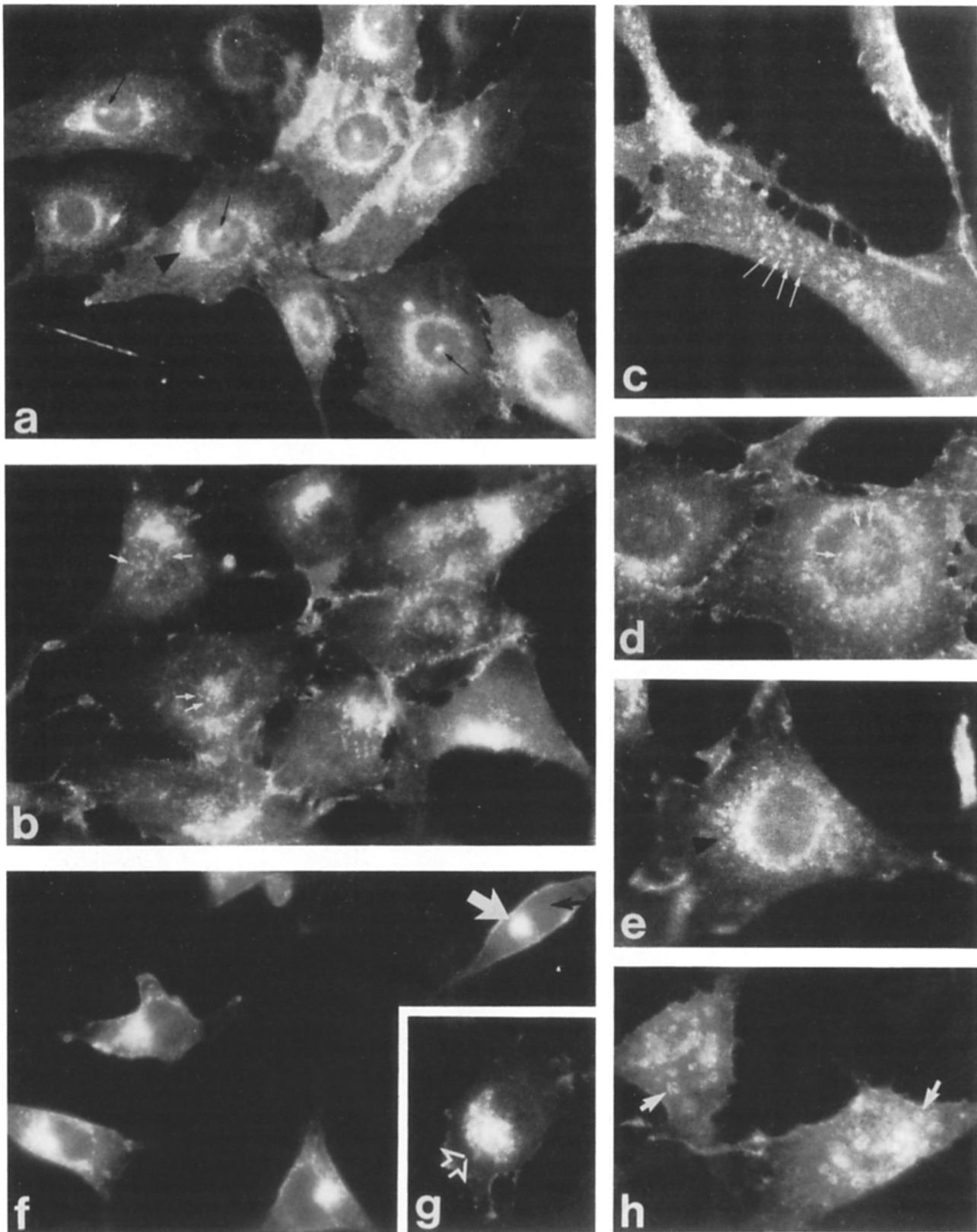
Figure 7. Fluorescence patterns of pp60^{c-src} obtained with mAb 327 after exposure of the c-*src* overexpresser cells to unlabeled Con A for various times. The focus was set at the cell bottom in *a, b, d, g,* and *h*; at the mid cell level in *e* and *f*; at the upper cell surface level in *c*. Initially pp60^{c-src} (*a*) exhibits the characteristic features explicated in the first section. After 15 min of exposure to the lectin, tiny dots containing pp60^{c-src} appear at the upper and lower cell surfaces (*small arrows* in *b, c,* and *d*). A perinuclear cluster of pp60^{c-src}-containing patches is still observed (*e*) as in untreated cells. After 1 h of exposure to Con A, a diffuse pp60^{c-src} fluorescence is seen inside the cytoplasm (*black arrow* in *f*) and a large cap made up of a number of pp60^{c-src}-containing patches is present inside the cell in a juxtanuclear position (*white arrow* in *f*) and also in part at the lower cell surface (*open arrow* in *g*). In some instances, instead of a cap, small aggregates of pp60^{c-src}-containing dots are situated on the lower cell surface (*h*). (*7a, b, f–h*) ×500; *7c–e*) ×700.

diffuse and patchy inside the cytoplasm. In these cells, a low level of plasma membrane-associated F-Con A is found initially present and also after 15 min of incubation with the lectin (*arrowheads*, Fig. 9, *k* and *l*). In the latter case, a few sparse intracellular patches containing both pp60^{c-src} and F-Con A may sometimes be observed (*small black arrows*, Fig. 9, *k* and *l*). As cells progress through mitosis and reach telophase a strong uniform Con A fluorescence appears at the cell surface, shortly after the addition of the lectin (*arrowhead*, Fig. 9 *n*). Later on, this surface-associate Con A internalizes and condenses together with pp60^{c-src} around newly formed MTOCs and at the distal ends of the midbody microtubules (*arrows*, Fig. 9, *o* and *p*) where Golgi elements also accumulate (Burke et al., 1982).

Discussion

Localization of pp60^{c-src} in Interphase c-src Overexpresser Cells: Involvement of pp60^{c-src} in Cellular Adhesion

The mouse mAb, mAb 327 (Lipsich et al., 1983) that recognizes specifically both pp60^{v-src} and pp60^{c-src} in a wide variety of cells, has been used to determine precisely the various locations of pp60^{c-src} in c-*src* overexpresser cells, the NIH (pMc-*src*/focus)B cells from Shalloway et al. (1984), using the technique of immunofluorescence microscopy. The immunolabeling of interphase cells show several characteristic features: (*a*) a uniformly dispersed fluorescence covering the inner cell surface; (*b*) a compact juxtanuclear spot located at the focal point of interphase microtubules where the centriole pair is also situated; and (*c*) a cluster of small patches embedded in a meshwork of microtubules that encompasses the nucleus more or less.

It is unlikely that the fluorescence detected with the mAb 327 could be due to antibody cross-reaction with other cellular proteins rather than to the c-*src* protein itself for several reasons: (*a*) the mAb 327 detects specifically only one 60-kD protein in a variety of cells when it is assayed either by immunoblot or by immunoprecipitation (Lipsich et al., 1983; our own results); (*b*) if the mAb 327 was cross-reacting with another cellular protein than pp60^{c-src} in immunofluorescence, we would expect that cross-reacting protein to be recognized as well in normal NIH 3T3 cells, which is not the case (Fig. 1 *a*); (*c*) no staining was observed when irrelevant mAbs are substituted for mAb 327 (not shown). It is equally unlikely that the pp60^{c-src} location patterns obtained with the mAb 327 are peculiar to the particular cell line used here since Kaplan et al. (1990; Kaplan, K. B., H. E. Varmus, and D. O. Morgan, personal communication) have described similar pp60^{c-src} distributions in COS7 cells and in RAT-1 fibroblasts overexpressing the chicken pp60^{c-src}. The possibility also must be considered that the localization of an overexpressed chicken pp60^{c-src} in mouse cells does not reflect the true location of the endogeneous mouse pp60^{c-src}. This, however, is improbable since the cellular *src* gene has been shown to be structurally highly conserved during evolution from sponges to mammalian cells (Barnekow and Schartl, 1984) and, since a second mAb, GD11, that has been shown to be directed against a highly conserved epitope of the molecule (Parsons et al., 1984, 1986) give pp60^{c-src} patterns quite similar to the mAb 327.

pp60^{c-src} also accumulates, often but not always, in the long cellular processes that develop when the cells are plated at low density. The formation of such processes, however, is inhibited when the cells are plated at high density or when they are plated at low density on a confluent layer of irradiated NIH 3T3 cells. In nearly confluent cultures, concentration of pp60^{c-src} can be observed at cell-contact areas. Such intercellular contacts, however, do not seem to be stable since, very often, the margin of one cell spreads out over the other. This phenomenon is consistent with observations reported by others that pp60^{c-src} overexpression reduces cell-adhesion (Warren and Nelson, 1987) and cell-cell communication (Azarnia et al., 1988). It is worthwhile to mention that pp60^{c-src} overexpression appears to mimic here the effect of pp60^{v-src} since it has been reported that pp60^{v-src} also impairs cell-cell communication (Chang et al., 1985; Crow et al., 1990). The presence of the long cellular processes filled with pp60^{c-src} in the NIH (pM c-*src*/focus)B cells plated at low density is also indicative of a lack of adhesive strength between these cells and the substratum. Indeed, strong adhesion between cells and substratum results in spreading of the cells concomitant with the appearance of well-developed actin cables and adhesion plaques. The formation of long cellular processes that results from pp60^{c-src} overexpression is most striking in MDCK cells, which are epithelial cells and, therefore, exhibit usually a typical polygonal shape (Warren et al., 1988). It has been shown that the neuronal form of pp60^{c-src} concentrates in the membranes of nerve growth cones, the motile structures of the developing neurones that are involved in neurite extension (Sobue and Konda, 1988; Maness et al., 1988). It is conceivable that strong cell-substratum adhesion would inhibit motility. In summary, a consistent feature stemming from a number of different works suggests that pp60^{c-src} functions in part to modulate cellular adhesion and motility.

Differential Distribution Patterns of pp60^{c-src} in c-src Overexpresser Cells and of pp60^{v-src} in RSV-transformed Cells

The next point we shall discuss is in what aspects the localization patterns of pp60^{c-src} differ from those of pp60^{v-src} when the two proteins are expressed at nearly equivalent levels. Fig. 10 shows a comparative picture of the localization patterns of pp60^{c-src} and of pp60^{v-src}, respectively, in the NIH (pM c-*src*/focus)B cells from Shalloway et al. (1984) and in RSV-transformed NIH 3T3 cells from our laboratory using the mAb 327. The localization of pp60^{v-src} in RSV-transformed cells has been as thoroughly studied by biochemical tools as by immunofluorescence in a variety of avian and mammalian cells (for review see Jove and Hanafusa, 1987). The viral protein exhibits in part a plasma membrane association (Willingham et al., 1979), situated essentially in residual adhesion plaques at the cell periphery (*thin white arrows*, Fig. 10 *b*; Rohrschneider, 1979; Nigg et al., 1982), intercellular contact areas (*white arrowhead*, Fig. 10 *b*; Krueger et al., 1980) and rosette components (*wide white arrows*, Fig. 10 *b*; Nigg et al., 1982), all cellular structures that are tightly linked with the nonionic, detergent-insoluble cytoskeletal matrix (Burr et al., 1980). In that respect, the viral and cellular proteins differ dramatically, since this study found no accumulation of pp60^{c-src} in adhe-
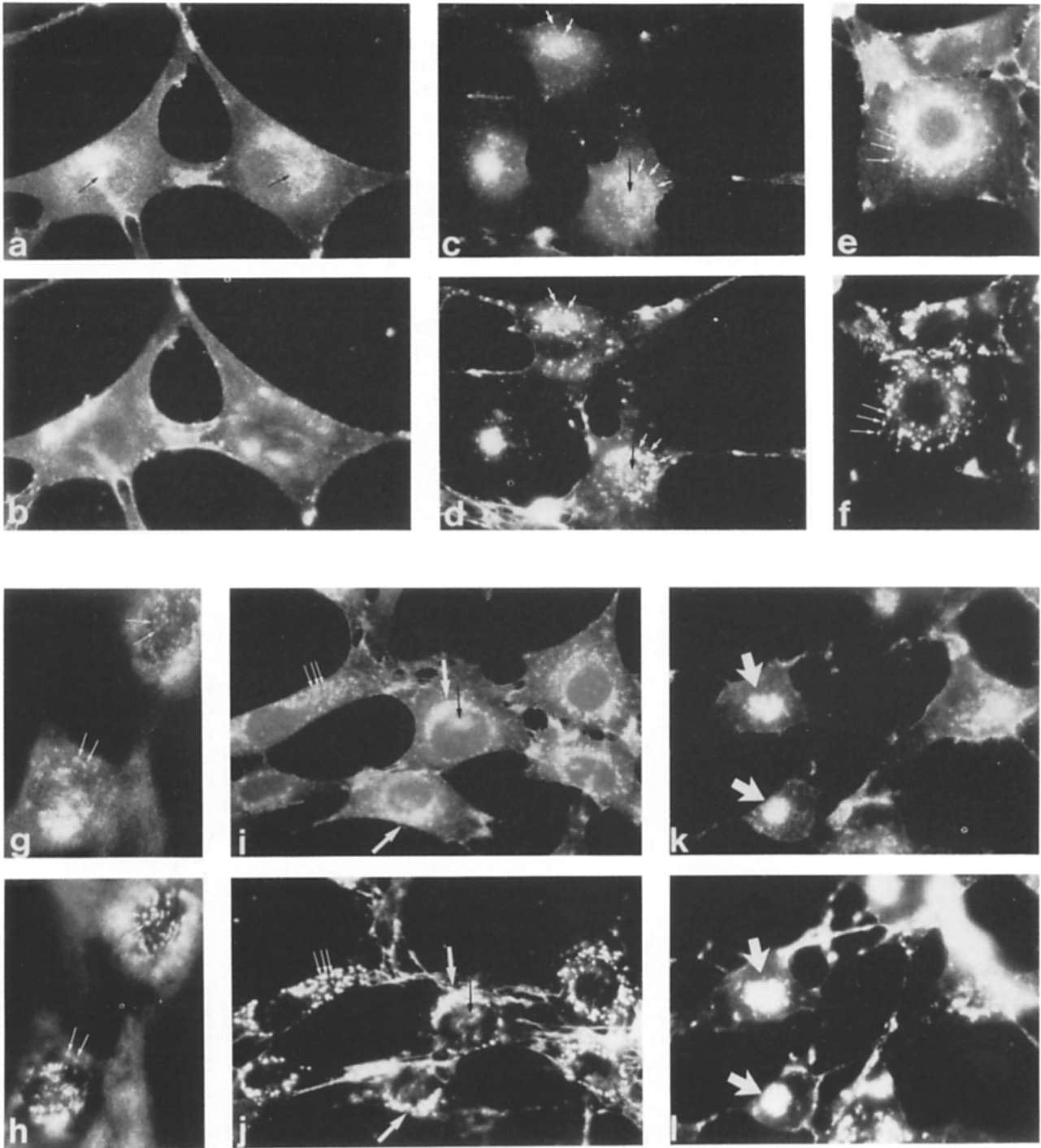
Figures 8 and 9. Simultaneous fluorescence patterns of F-Con A (Fig. 8, *b, d, f, h, j,* and *l;* Fig. 9, *b, d, f, h, j, l, n,* and *p*) and pp60$^{c\text{-}src}$ (Fig. 8, *a, c, e, g, i,* and *k;* Fig. 9, *a, c, e, g, i, k, m,* and *o*) on the same cells following exposure of c-*src* overexpresser NIH 3T3 cells to F-Con A for various times. (Fig. 8, *a* and *b*) initial patterns. (Fig. 8, *c, d, e, f, g, h, i,* and *j*) pairs of pictures showing patterns observed after 15 min incubation with the fluorescent lectin. The thin arrows point to patches labeled with the two reagents and located either at the lower cell surface level (Fig. 8, *c* and *d*) or at upper cell surface level (Fig. 8, *e, f, g, h, i,* and *j*). The wide arrows in *i* and *j* show perinuclear clusters of patches labeled with F-Con A and for pp60$^{c\text{-}src}$. A localization of pp60$^{c\text{-}src}$ in the centriolar region from which F-Con A is excluded may be observed *(thin black arrows* in Fig. 8, *c* and *d* and *i* and *j*). (Fig. 8, *k, l* and Fig. 9, *a–f*) pairs of pictures showing the localization patterns of F-Con A and pp60$^{c\text{-}src}$ after 1 h of exposure to the lectin. A juxtanuclear cap containing both components is seen inside the cells *(wide white arrows* in Fig. 8, *k* and *l* and Fig. 9, *a–d*) with a part located at the lower cell surface level (Fig. 9, *e* and *f*). Some surface staining remains occasionally *(arrowheads,* Fig. 9, *a* and *b*) together with a diffuse intracellular staining *(black arrows,* Fig. 9, *c* and *e*) and a centrosomal one for pp60$^{c\text{-}src}$ only *(thin white arrows,* Fig. 9, *e* and *f*). In mitotic cells (Fig. 9, *g–p*), before the G2 to M transition, the initially uniformly dispersed Con A fluorescence that stands at the cell surface (Fig. 9 *h*) becomes integrated in the region surrounding the two diplosomes *(black arrows,* Fig. 9 *j*) in which concentrates pp60$^{c\text{-}src}$ initially (Fig. 9 *g*) and after 15 min incubation with F-Con A *(black arrows,* Fig. 9 *i*). Between prophase to anaphase, initially and after 15 min incubation with F-Con A, pp60$^{c\text{-}src}$ remains essentially diffusely distributed inside the cells *(black arrow,* Fig. 9 *k*) and a low level of F-Con A appears mainly plasma membrane-associated *(arrowhead,* Fig. 9 *l*). A limited number of intracellular patches containing both F-Con A and pp60$^{c\text{-}src}$ *(small black arrows* in Fig. 9, *k* and *l*) may sometimes appear after 15 min incubation with the lectin. A strong concentration of F-Con A staining
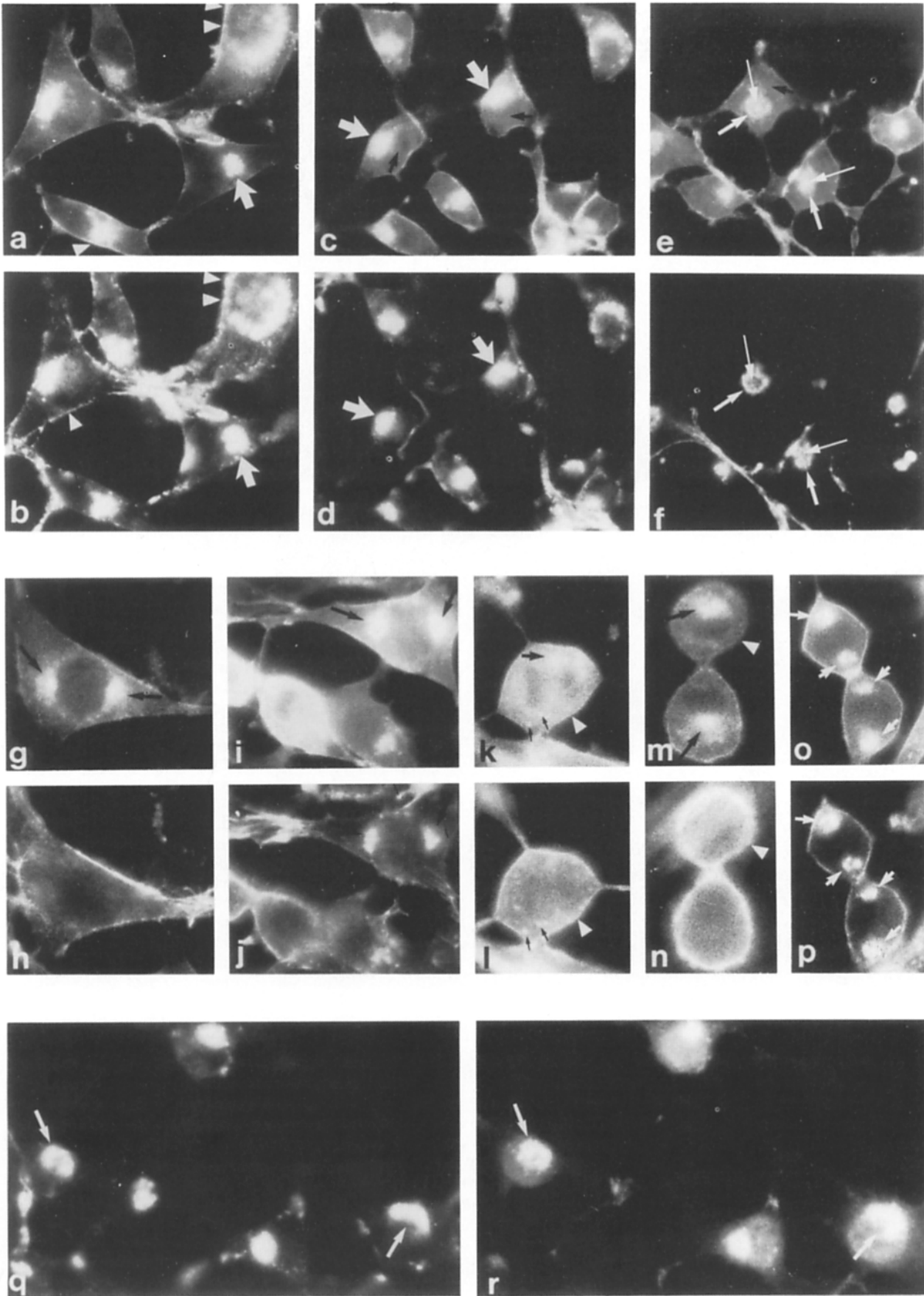
reappears at the surface of the cells in early telophase (*arrowhead*, Fig. 9 *n*) shortly after the addition of the lectin. After 15 min incubation, F-Con A becomes again internalized in the MTOC region and at the distal ends of midbody microtubules where also pp60[c-src] concentrates (*arrows* in Fig. 9, *o* and *p*). In Fig. 9, *q* and *r*, after 1 h incubation with F-Con A, the intracellular part of the F-Con A (*arrows* in Fig. 9 *q*) and pp60[c-src]-containing cap coincide with the Golgi apparatus visualized with fluorescent wheat germ agglutinin (Virtanen et al., 1980; *arrows* in Fig. 9 *r*). Fig. 8, *a–f*, *i–l*; Fig. 9, *a–f*, ×300; Fig. 8, *g* and *h*; Fig. 9, *g–r*, ×500.

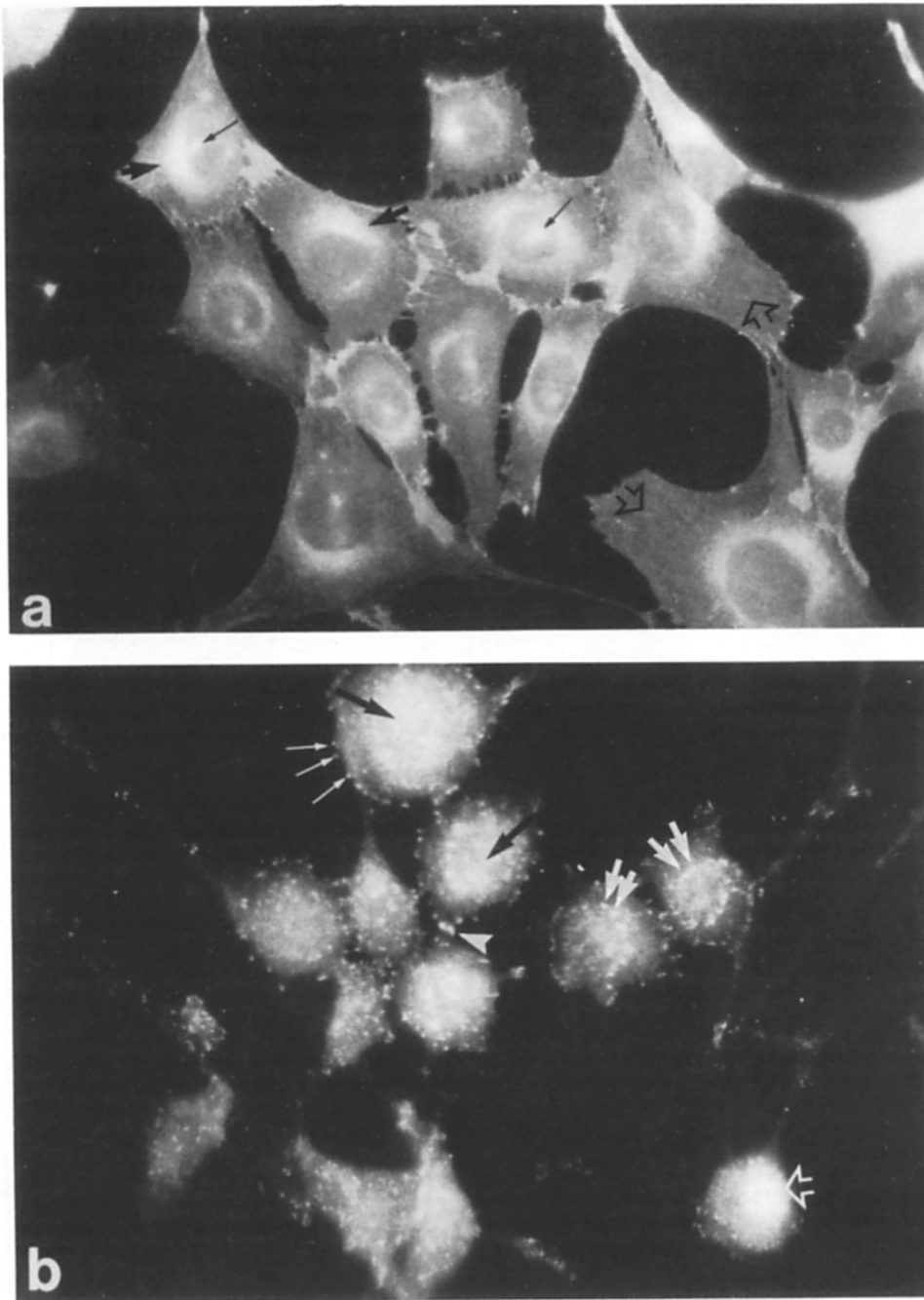*Figure 10.* Comparative picture showing the pp60$^{c\text{-}src}$ distribution in NIH (pM c-src/focus)B cells (*a*) and the pp60$^{v\text{-}src}$ distribution in RSV-transformed NIH 3T3 cells (*b*) after immunolabeling with the mAb 327. The following features are pointed out: in *a*, the compact juxtanuclear pp60$^{c\text{-}src}$-containing spot (*thin arrows*), the perinuclear cluster of pp60$^{c\text{-}src}$-containing patches (*wide black arrows*), the uniform plasma membrane-associated pp60$^{c\text{-}src}$ fluorescence (*open arrows*); in *b*, a diffuse cytoplasmic pp60$^{v\text{-}src}$ fluorescence (*black arrows*), pp60$^{v\text{-}src}$-containing residual adhesion plaques at the cell periphery (*thin arrows*), pp60$^{v\text{-}src}$-containing rosette components at the inner ventral cell surface (*wide white arrows*), pp60$^{v\text{-}src}$ staining of an intercellular contact area (*white arrowhead*), a juxtanuclear accumulation of diffuse pp60$^{v\text{-}src}$ fluorescence (*open arrow*). ×400.

sion plaques nor in rosettes. These latter structures appear to be specific for RSV-transformed cells and, besides pp60$^{v\text{-}src}$, a number of cytoskeletal proteins including actin, α-actinin, vinculin, and talin have been shown to concentrate in them (review in Burridge et al., 1988). Overexpression of pp60$^{c\text{-}src}$, therefore, is unable to lead to a disorganization of the actin skeleton and of the adhesion plaques as pp60$^{v\text{-}src}$ expression does.

Also, in contrast with pp60$^{v\text{-}src}$, pp60$^{c\text{-}src}$ is rather uniformly distributed at the inner face of the plasma membrane (*open arrows*, Fig. 10 *a*). A diffuse intracellular pp60$^{v\text{-}src}$ distribution is also observed in many transformed cells (*black arrows*, Fig. 10 *b*; Nigg et al., 1982). An equivalent pp60$^{c\text{-}src}$ diffuse distribution is generally not found in inter-

phase cells but it becomes a major distribution of pp60$^{c\text{-}src}$ in mitotic cells.

Using the α p60 serum, Resh and Erikson (1985) detected a pp60$^{v\text{-}src}$ population in juxtareticular nuclear membranes, that could be visualized by immunofluorescence microscopy in RSV-transformed vole cells. This intracellular staining was also observed using TBR sera (Rohrschneider, 1979) and rabbit antibodies against a synthetic peptide containing the six terminal amino acids of pp60$^{v\text{-}src}$ (Nigg et al., 1982). Using the mAb 327, the same type of bright juxtanuclear diffuse staining can sometimes be observed (*open arrow*, Fig. 10 *b*). In contrast, a juxtanuclear pp60$^{c\text{-}src}$ population present as small patches or vesicles is frequently observed in the c-src overexpresser cells. Moreover, the characteristic

centriolar pp60$^{c\text{-}src}$ spot of fluorescence has no counterpart for pp60$^{v\text{-}src}$ in the SRD-NIH 3T3 cells.

There is apparently only one cellular site for which the two proteins exhibit a similar affinity, this is the intercellular contact areas. It is interesting to note that the two proteins appear to exert here the same function in reducing intercellular adhesion and communication (Warren and Nelson, 1987; Azarnia et al., 1988; Chang et al., 1985; Crow et al., 1990).

In summary, pp60$^{v\text{-}src}$ and pp60$^{c\text{-}src}$ seem to interact with a high affinity with quite different cellular targets. A membrane association that depends in part on the covalent linkage of fatty acid myristate to the amino terminus of the molecules appears to be required for transformation by pp60$^{v\text{-}src}$ (Cross et al., 1984; Kamps et al., 1985). The same kind of plasma membrane association occurs with pp60$^{c\text{-}src}$ without transformation even at a high pp60$^{c\text{-}src}$ level of expression. In fact, the two proteins do not exhibit the same location at the plasma membrane level (Fig. 10). pp60$^{v\text{-}src}$ has been shown recently (Kaplan et al., 1990) to contain independent amino-terminal domains that are specific for attachment to different cellular targets. The viral and cellular *src* proteins differ in their amino acid sequence, including regions in their amino-terminal domain. It would certainly be of interest to determine the domain(s) amongst the structural differences between pp60$^{v\text{-}src}$ and pp60$^{c\text{-}src}$ that is (are) responsible for their differential binding to the plasma membrane and how such a difference affects the interaction of the proteins towards the plasma membrane.

An observation that emerges from this study deserves to be noted here: when the NIH (pM c-*src*/focus)B cells are exposed to Con A for 15 min, the initial pp60$^{c\text{-}src}$ distribution changes, becoming more similar to the distribution of pp60$^{v\text{-}src}$ in RSV-transformed cells; in particular, a diffuse cytoplasmic fluorescence starts to appear and a clustering of small round patches that remind those present in the pp60$^{v\text{-}src}$-containing rosettes, occurs in particular at the inner ventral cell surface. A possible interpretation, amongst alternative ones, could be that pp60$^{v\text{-}src}$, after binding to the inner side of the plasma membrane, spontaneously induces the patching of cell surface molecules in the absence of external stimuli and, subsequently, the rosette formation at the ventral cell surface. Further work is needed to test such a hypothesis.

Localization of pp60$^{c\text{-}src}$ in Premitotic and Mitotic c-src Overexpresser Cells

Here we discuss the fate of pp60$^{c\text{-}src}$ during the premitotic and mitotic phases. A considerable redistribution of pp60$^{c\text{-}src}$ takes place during these phases, particularly at the G2-M phase transition, at which time the plasma membrane-associated pp60$^{c\text{-}src}$ fluorescence becomes patchy, a diffuse cytoplasmic pp60$^{c\text{-}src}$ fluorescence breaks through, and a strong agglutination of pp60$^{c\text{-}src}$-containing patches occurs around the two diplosomes. From prophase to metaphase, the two prominent distributions of pp60$^{c\text{-}src}$ that are observed throughout the cells are diffuse and patchy inside the cytoplasm and the two pericentriolar pp60$^{c\text{-}src}$ clusters tend to dissolve. During anaphase and in early telophase, the main intracellular pp60$^{c\text{-}src}$ fluorescence is rather diffuse and a new finely punctuated pp60$^{c\text{-}src}$ fluorescence appears at the level of the cell surface. Late in telophase, the cell surface fluorescence intensifies and pp60$^{c\text{-}src}$ starts concentrating again in the MTOC regions of the two daughter cells.

The second part of Results, which shows an apparent association of pp60$^{c\text{-}src}$ with vesicles containing Con A-receptor complexes, suggests that intracellular pp60$^{c\text{-}src}$-containing patches in interphase cells may represent endocytosed plasma membrane vesicles (endosomes) to which pp60$^{c\text{-}src}$ molecules are associated and that have been vehiculated along the interphase microtubules up to the centrosome. The appearance of a plasma membrane-associated pp60$^{c\text{-}src}$ patching together with the accumulation of pp60$^{c\text{-}src}$-containing patches around the two centriole pairs in the late G2 phase is consistent with this hypothesis. Indeed, the rate of plasma membrane endocytosis has to be greatly enhanced before mitosis for the cell to round up. The ensuing dissolution of the two pericentriolar pp60$^{c\text{-}src}$ clusters which starts at early prophase occurs concomitant with a depolymerization of the aster microtubules and growth of the spindle. This observation indicates that the preferential association of pp60$^{c\text{-}src}$ with the material surrounding the centrioles is lost following the breakdown of the nuclear envelope and the beginning of spindle formation. The p34^{cdc2} protein kinase, a major cell cycle regulatory kinase (for reviews see Dunphy et al., 1988; Murray, 1988; Lee and Nurse, 1988; Gautier et al., 1988) has been shown to be a nuclear and cytoplasmic protein with a cell cycle-dependent accumulation at the centrosome (Akhurst et al., 1979; Bailly et al., 1989), although a strictly nuclear localization has been reported by others (Riabowol et al., 1989). This protein is capable in vitro of phosphorylating pp60$^{c\text{-}src}$ at the same sites as those phosphorylated in vivo during fibroblast mitosis (Chakalaparampil and Shalloway, 1988; Shenoy et al., 1989; Morgan et al., 1989). p34^{cdc2} can be itself phosphorylated on serine, threonine and tyrosine residues and threonine/tyrosine dephosphorylation accompanies its activation during entry to mitosis (Morla et al., 1989). It is not clear, however, if pp60$^{c\text{-}src}$ is the protein kinase responsible for the tyrosine phosphorylation of the p34^{cdc2} protein in vivo (Draetta et al., 1988; Shenoy et al., 1989; Morgan et al., 1989). In any case, a necessary, although not sufficient, condition for a protein kinase to be able to phosphorylate a physiological substrate in vivo, is that this protein kinase interacts physically and specifically with its substrate at (a) common cellular localization site(s). pp60$^{c\text{-}src}$ and p34^{cdc2} appear, at least in part, as two centrosomal proteins. Therefore, they would be able to interact in vivo in the region of the centrosome. Such an interaction might be responsible for the appearance of novel serine and threonine phosphorylation sites in pp60$^{c\text{-}src}$ and operate at the G2 to M phase transition to dissolve the pp60$^{c\text{-}src}$-containing pericentriolar material that would end up by the loss of interaction between the p34^{cdc2} protein and pp60$^{c\text{-}src}$. The possibility, therefore, cannot be excluded that such a dissociation might be required to allow mitotic activation of the p34^{cdc2} protein kinase and entry in mitosis.

Besides this delocalization of pp60$^{c\text{-}src}$ from the centriolar area, another drastic change in the distribution patterns of pp60$^{c\text{-}src}$ occurs at the G2-M transition. It is the appearance of a diffuse fluorescence that seems to counterbalance the disappearance of the plasma membrane-associated one. At the same mitotic stage, the process of internalization of Con A-receptor complexes is greatly reduced (last section of Results). It is known that endocytotic processes are profoundly depressed during mitosis (Berlin et al., 1978). If pp60$^{c\text{-}src}$ is involved in such processes, it may be possible

that this function requires a plasma membrane association and that endocytosis will be inhibited after delocalization of pp60$^{c\text{-}src}$ from the plasma membrane to the cytoplasm. Of course, the possibility remains that plasma membrane pp60$^{c\text{-}src}$ delocalization and depression of endocytotic processes during mitosis are unrelated.

The last observation of a faint fibrillar pp60$^{c\text{-}src}$ staining between the spindle poles during prometaphase and metaphase may be interpreted as representing pp60$^{c\text{-}src}$-containing vesicles migrating along interpolar microtubules.

Possible Involvement of pp60$^{c\text{-}src}$ in Endocytotic Processes

The binding of Con A to the surface of normal and c-src overexpresser cells induced the patching, internalization, and capping of the Con A receptors. This study shows that, at each stage of this endocytotic process, the overall Con A pattern coincides with a part of the pp60$^{c\text{-}src}$ pattern in the NIH (pM c-src/focus)B cells: (a) initially, both the lectin and a fraction of the pp60$^{c\text{-}src}$ molecules exhibit a uniformly dispersed distribution at the cell surface level (outside for F-Con A, inside for pp60$^{c\text{-}src}$; (b) then, when Con A patches form at the surface of the cells and start to internalize and accumulate around the nucleus, pp60$^{c\text{-}src}$ patches also emerge which superimpose on the Con A patches; (c) finally as the Con A patches coalesce into a single central cap, coincident with the Golgi apparatus, a pp60$^{c\text{-}src}$ cap that superimposes on the Con A cap is also observed.

Parallel to the pp60$^{c\text{-}src}$ and Con A copatching that occurs when the cells are exposed for 15 min to the fluorescent lectin, the compact, juxtanuclear pp60$^{c\text{-}src}$-containing spot tends to disaggregate. Also, a perinuclear cluster of pp60$^{c\text{-}src}$ patches similar to that observed in untreated cells is still observed after 15 min of exposure to F-Con A, but, in that latter case, the patches are also labeled with the fluorescent lectin. This observation suggests that, after the binding of F-Con A molecules to their receptors at the cell surface, the Con A–receptor complexes internalize and integrate pp60$^{c\text{-}src}$-containing structures that are translocated rapidly to the region of the centrosome.

Processing of the cells with F-Con A at 37°C for 1 h results in the formation of caps that locate near the cell center and are labeled both for pp60$^{c\text{-}src}$ and with F-Con A. One part of the cap that apparently localizes at the cell–substratum interface also stains for actin. The inner part of the cap, which coincides with the Golgi apparatus and the centrosome, does not stain for actin. Two major differences between the overall pp60$^{c\text{-}src}$ and Con A patterns can be pointed out at this endocytotic stage: (a) concomitant to the pp60$^{c\text{-}src}$- and Con A–cap formation and to the disappearance of the plasma membrane-associated, uniform pp60$^{c\text{-}src}$ and Con A fluorescences, a diffuse pp60$^{c\text{-}src}$, but not Con A, staining breaks through the cytoplasm; (b) when the resolution is good enough, a dense spot that always stains for pp60$^{c\text{-}src}$, but never stains for F-Con A, may be observed right in the middle of the cap. Such a spot probably represents the pericentriolar area from which Golgi elements are excluded. These observations indicate that the capping of patches containing both pp60$^{c\text{-}src}$ and Con A occurs within the Golgi apparatus or in a compartment intimately linked to the Golgi complex. During this capping process, pp60$^{c\text{-}src}$-containing vesicles keep on accumulating in the centriolar area, as in interphase,

untreated cells. In other words, the intracellular compartment to which the pp60$^{c\text{-}src}$-containing vesicles will be transported depends on whether these vesicles have associated Con A–receptor complexes or not. A similar situation has been described recently by Koval and Pagano (1989). These authors have shown that sphingomyelin, a major lipid component of the plasma membrane, transits through the pericentriolar area before recycling to the plasma membrane, whereas its hydrolyzed form is transported to the Golgi apparatus where new sphingomyelin is synthesized before recycling. It is easy to conceive that, in our system, components of the pp60$^{c\text{-}src}$-containing vesicles are modified by their association to Con A–receptor complexes. This would explain why, the pp60$^{c\text{-}src}$- and Con A–associated vesicles may have to transit via the Golgi apparatus where the pp60$^{c\text{-}src}$-containing vesicles destined for the plasma membrane will be reconstituted.

After 20 min of exposure of normal rat kidney or WI38 human cells to Con A or to antibodies directed against different integral proteins, the binding of these reagents to their respective receptors at the cell surface has been shown to induce these receptors to redistribute to a limited extent into patches situated at the cell surface (Ash and Singer, 1976; Ash et al., 1977). By contrast, the binding of a multivalent ligand to its specific receptors on the surface of many cell in suspension, including lymphocytes, results first in a clustering of the receptors in small patches at the cell surface and, then, aggregation of the patches into a single cap (reviewed in Ash et al., 1977). Ash et al. suggested that the ligand receptor patches were immobilized as a result of their association to stress fibers underlying the plasma membrane in fibroblasts, whereas, in lymphocytes, which do not possess stress fibers, such patches may move in the plane of the membrane and collect into a cap. In the NIH 3T3 cells, we observed that the actin cables were breaking down after the binding of Con A to the cell surface. This phenomenon could explain why, like in lymphocytes, capping of the Con A patches may occur in the mouse cells. Other cultured cells, ovarian granulosa cells (Albertini and Anderson, 1977) have been shown to behave as the NIH 3T3 cells here.

At each stage of the Con A–mediated endocytotic process, the Con A patterns are similar for the normal and the c-src overexpresser NIH 3T3 cells. This indicates that the quantity of pp60$^{c\text{-}src}$ associated to the vesicles, which incorporate the Con A–receptor complexes, does not affect the process.

pp60$^{c\text{-}src}$ behaves as an integral membrane protein that is located on the inner cell surface and does not span the cell membrane, exhibiting a portion of it on the external cell surface as many transmembrane glycoproteins. Therefore, it is not itself a glycoprotein that could bind a lectin like Con A or WGA. Yet, after the binding of a lectin (WGA as well as Con A) to the oligosaccharide moieties of transmembrane glycoproteins, patches and caps containing the lectin–receptor complexes form to which pp60$^{c\text{-}src}$ appears to be associated. Such a phenomenon appears to be specific to pp60$^{c\text{-}src}$ since it does not occur with p21^{ras}, another protooncogene product anchored to the cytoplasmic face of the plasma membrane (unpublished results). One may question, however, whether the endocytotic process induced by the binding of single defined ligands such as mitogens and antigens to their specific receptors really occurs via a mechanism similar to the Con A–induced process. We show here that, by 15 min, the F-Con A–receptor complexes start con-

centrating in the centrosomal area. Such a time schedule is the same as that followed by the EGF–receptor complexes, which have been shown recently to be carried in the pericentriolar area of epidermoid carcinoma cells after entering multivesicular bodies moving along a tubular reticulum (Hopkins et al., 1990). The Con A–receptor complexes could be internalized and processed towards the centrosome via a mechanism similar to that functioning for the EGF–receptor complexes. In summary, if this study does not demonstrate directly that pp60$^{c\text{-}src}$ plays an active role in endocytotic processes, it raises the question what pp60$^{c\text{-}src}$ is doing along the endocytotic pathway of the Con A–receptor complexes. It is worthwhile here to recall that pp60$^{c\text{-}src}$ has been implicated in the reverse process of exocytosis (Parsons and Creutz, 1986; Grandori and Hanafusa, 1988).

References

Akhurst, R. J., N. B. Flavin, J. Worden, and M. G. Lee. 1989. Intracellular localization and expression of mammalian CDC2 protein during myogenic differentiation. *Differentiation.* 40:36–41.

Albertini, D. F., and E. Anderson. 1977. Microtubule and microfilament rearrangements during capping of concanavalin A-receptors on cultured ovarian granulosa cells. *J. Cell. Biol.* 73:109–127.

Ash, J. F., and S. J. Singer. 1976. Concanavalin A-induced transmembrane linkage of concanavalin A surface receptors to intracellular myosin-containing filaments. *Proc. Natl. Acad. Sci. USA.* 73:4575–4579.

Ash, J. F., D. Louvard, and S. J. Singer. 1977. Antibody-induced linkage of plasma membrane proteins to intracellular actomyosin-containing filaments in cultured fibroblasts. *Proc. Natl. Acad. Sci. USA.* 74:5584–5588.

Azarnia, R., S. Reddy, T. E. Kmiecik, D. Shalloway, and W. R. Loewenstein. 1988. The cellular src gene product regulates junctional cell to cell communication. *Science (Wash. DC).* 239:398–401.

Bailly, E., M. Doree, P. Nurse, and M. Bornens. 1989. p34^{cdc2} is located in both nucleus and cytoplasm: part is centrosomally associated at G2/M and enter vesicles at anaphase. *EMBO (Eur. Mol. Biol. Organ.) J.* 8:3985–3995.

Barak, L. S., R. R. Yocum. E. A. Nothnagel, and W. W. Webb. 1980. Fluorescence staining of the actin cytoskeleton in living cells with 7-nitrobenz-2-oxo-1,3-diazole phallacidin. *Proc. Natl. Acad. Sci. USA.* 77:980–984.

Barnekow, A., and M. Schartl. 1984. Cellular src gene product detected in the fresh water sponge *Spongilla lacustris. Mol. Cell. Biol.* 4:1179–1181.

Barnekow, A., R. Jahn, and M. Schartl. 1990. Synaptophysin: a substrate for the protein kinase pp60$^{c\text{-}src}$ in intact synaptic vesicles. *Oncogene.* 5:1019–1024.

Berlin, R. D., J. M. Oliver, and R. J. Walter. 1978. Surface functions during mitosis I: phagocytosis, pinocytosis and mobility of surface bound ConA. *Cell.* 15:327–341.

Brinkley, B. R., G. M. Fuller, and D. P. Highfield. 1975. Cytoplasmic microtubules in normal and transformed cells in culture: analysis by tubulin antibody immunofluorescence. *Proc. Natl. Acad. Sci. USA.* 72:4981–4985.

Brugge, J. S., W. Yonemoto, and D. Darrow. 1983. Interaction between the Rous sarcoma virus transforming protein and two cellular phosphoproteins: analysis of the turnover and distribution of this complex. *Mol. Cell. Biol.* 3:9–19.

Burke, R., G. Griffiths, H. Raggio, D. Louvard, and G. Warren. 1982. A monoclonal antibody against a 135 K Golgi membrane protein. *EMBO (Eur. Mol. Biol. Organ.) J.* 1:1621–1628.

Burr, J. G., G. Dreyfuss, S. Penman, and J. Buchanan. 1980. Association of the src gene product of Rous sarcoma virus with cytoskeletal structures of chicken embryo fibroblasts. *Proc. Natl. Acad. Sci. USA.* 77:3484–3488.

Burridge, K. 1976. Changes in cellular glycoproteins after transformation: identification of specific glycoproteins and antigens in sodium dodecylsulfate gels. *Proc. Natl. Acad. Sci. USA.* 73:4457–4461.

Burridge, K., K. Fath, T. Telly, G. Nuckolls, and C. Turner. 1988. Focal adhesions: transmembrane junctions between the extracellular matrix and the cytoskeleton. *Annu. Rev. Cell. Biol.* 4:487–525.

Chackalaparampil, I., and D. Shalloway. 1988. Altered phosphorylation and activation of pp60$^{c\text{-}src}$ during fibroblast mitosis. *Cell.* 52:801–810.

Chang, C.-C., J.-E. Trosko, H.-J. Kung, D. Bombick, and F. Matsumura. 1985. Potential role of the src gene product in inhibition of gap junctional communication in NIH/3T3 cells. *Proc. Natl. Acad. Sci. USA.* 82:5360–5364.

Courtneidge, S. A., A. D. Levinson, and J. M. Bishop. 1980. The protein encoded by the transforming gene of avian sarcoma virus and a homologous protein in normal cells are associated with the plasma membrane. *Proc. Natl. Acad. Sci. USA.* 77:3783–3787.

Cross, F. R., E. A. Garber, D. Pellman, and H. Hanafusa. 1984. A short sequence in the pp60^{src} N terminus is required for pp60^{src} myristylation and membrane association and for cell transformation. *Mol. Cell. Biol.* 6:1834–1842.

Crow, D. S., E. C. Beyer, D. L. Paul, S. S. Kobe, and A. F. Lau. 1990. Phosphorylation of Connexin 43 gap junction protein in uninfected and Rous sarcoma virus-transformed mammalian fibroblasts. *Mol. Cell. Biol.* 10:1754–1763.

David-Pfeuty, T., and S. J. Singer. 1980. Altered distributions of the cytoskeletal proteins vinculin and α-actinin in cultured fibroblasts transformed by Rous sarcoma virus. *Proc. Natl. Acad. Sci. USA.* 77:6687–6691.

Draetta, G., H. Piwnica-Worms, D. Morrison, B. Druker, T. Roberts, and D. Beach. 1988. Human cdc2 is a major cell-cycle regulated tyrosine kinase substate. *Nature (Lond.).* 336:738–743.

Dunphy, W. G., L. Brizuela, D. Beach, and J. Newport. 1988. The major *Xenopus* cdc2 protein is a component of MPF, a cytoplasmic regulator of mitosis. *Cell.* 54:423–431.

Ferrell, J. E., J. A. Noble, G. S. Martin, Y. V. Jacques, and D. F. Bainton. 1990. Intracellular localization of pp60$^{c\text{-}src}$ in human platelets. *Oncogene.* 5:1033–1036.

Gautier, J., C. Norbury, M. Lohka, P. Nurse, and J. Maller. 1988. Purified maturation-promoting factor contains the product of a Xenopus homolog of the fission yeast cell cycle control gene cdc2$^+$. *Cell.* 54:433–439.

Grandori, C., and H. Hanafusa. 1988. pp60$^{c\text{-}src}$ is complexed with a cellular protein in subcellular compartment involved in exocytosis. *J. Cell. Biol.* 107:2125–2135.

Hamaguchi, M., and H. Hanafusa. 1987. Association of pp60^{src} with Triton X-100 resistent cellular structure correlates with morphological transformation. *Proc. Natl. Acad. Sci. USA.* 84:2312–2316.

Hopkins, C. R. 1986. Membrane boundaries involved in the uptake and intracellular processing of cell surface receptors. *Trends Biochem. Sci.* 11:473–477.

Hopkins, C. R., A. Gibson, M. Shipman, and K. Miller. 1990. Movement of internalized ligand-receptor complexes along a continuous endosomal reticulum. *Nature (Lond.).* 346:335–339.

Hunter, T., and B. M. Sefton. 1980. The transforming gene product of Rous sarcoma virus phosphorylates tyrosine. *Proc. Natl. Acad. Sci. USA.* 77:1311–1315.

Iba, H., F. R., Takeya, T. Cross, T. Hanafusa, and H. Hanafusa. 1984. Rous sarcoma virus variants that carry the cellular src gene instead of the viral sec gene cannot transform chicken embryo fibroblasts. *Proc. Natl. Acad. Sci. USA.* 81:4424–4428.

Johnson, P. J., P. M. Coussens, A. V. Danko, and D. Shalloway. 1985. Overexpressed pp60$^{c\text{-}src}$ can induce focus formation without complete transformation of NIH 3T3 cells. *Mol. Cell. Biol.* 5:1073–1083.

Jove, R., and H. Hanafusa. 1987. Cell transformation by the viral src oncogene. *Annu. Rev. Cell. Biol.* 3:31–56.

Kamps, M. P., J. E. Buss, and B. M. Sefton. 1985. Mutation of NH₂-terminal glycine of pp60^{src} prevents both myristylation and morphological transformation. *Proc. Natl. Acad. Sci. USA.* 82:4625–4628.

Kaplan, J. M., H. E. Varmus, and J. M. Bishop. 1990. The src protein contains multiple domains for specific attachment to membranes. *Mol. Cell. Biol.* 10:1000–1009.

Koval, M., and R. E. Pagano. 1989. Lipid recycling between the plasma membrane and intracellular compartments: transport and metabolism of fluorescent sphingomyelin analogues in cultures fibroblasts. *J. Cell. Biol.* 108:2169–2181.

Krueger, J. G., E. Wang, E. A. Garber, and A. R. Goldberg. 1980. Difference in intracellular location of pp60^{src} in rat and chicken cells transformed by Rous sarcoma virus. *Proc. Natl. Acad. Sci. USA.* 77:4142–4146.

Lee, M., and P. Nurse. 1987. Complementation used to clone a human homologue of the fission yeast cell cycle control gene cdc2$^+$. *Nature (Lond.).* 327:207–208.

Lipsich, L. A., A. J. Lewis, and J. S. Brugge. 1983. Isolation of monoclonal antibodies that recognize the transforming protein of avian sarcoma viruses. *J. Virol.* 48:352–360.

Loeb, D. M., J. Woolford, and K. Beemon. 1987. pp60$^{c\text{-}src}$ has less affinity for the detergent-insoluble cellular matrix than do pp60$^{v\text{-}src}$ and other viral protein-tyrosine kinases. *J. Virol.* 61:2420–2427.

Louvard, D., H. Reggio, and G. Warren. 1982. Antibodies to the Golgi complex and the rough endoplasmic reticulum. *J. Cell. Biol.* 92:92–107.

Maness, P. F., M. Aubry, C. G. Shores, L. Frame, and K. H. Pfenninger. 1988. c-src gene product in developing rat brain is enriched in nerve growth cone membranes. *Proc. Natl. Acad. Sci. USA.* 85:5001–5005.

McIntosh, J. R., P. K. Hepler, and D. G. VanWie. 1969. Model for mitosis. *Nature (Lond.).* 224:659–663.

Morgan, D. O., J. M. Kaplan, J. M. Bishop, and H. E. Varmus. 1989. Mitosis-specific phosphorylation of pp60^{c-src} by p34^{cdc2}-associated protein kinase. *Cell.* 57:775-786.

Morla, A. O., G. Draetta, D. Beach, and J. Y. J. Wang. 1989. Reversible tyrosine phosphorylation of cdc2: dephosphorylation accompanies activation during entry in mitosis. *Cell.* 58:193-203.

Murray, A. W. 1988. A mitotic inducer matures. *Nature (Lond.).* 335:207-208.

Nigg, E. A., B. M. Sefton, T. Hunter, G. Walter, and S. J. Singer. 1982. Immunofluorescence localization of the transforming protein of Rous sarcoma virus with antibodies against a synthetic src peptide. *Proc. Natl. Acad. Sci. USA.* 79:5322-5326.

Parker, R. C., H. E. Varmus, and J. M. Bishop. 1984. Expression of v-src and chicken c-src in rat cells demonstrates qualitative differences between pp60^{v-src} and pp60^{c-src}. *Cell.* 37:131-139.

Parsons, S. J., and C. E. Creutz. 1986. pp60^{c-src} activity detected in the chromaffin granule membrane. *Biochem. Biophys. Res. Commun.* 134:736-742.

Parsons, S. J., D. J. McCarley, C. M. Ely, D. C. Benjamin, and J. T. Parsons. 1984. Monoclonal antibodies to Rous sarcoma virus pp60^{src} react with enzymatically active cellular pp60^{src} of avian and mammalian origin. *J. Virol.* 51:272-282.

Parsons, S. J., D. J. McCarley, V. W. Raymond, and J. T. 1986. Localization of conserved and non conserved epitopes within the Rous sarcoma virus-encoded src protein. *J. Virol.* 59:755-758.

Rendu, F., M. Lebret, S. Danielen, R. Fagard, S. Levy-Toledano, and S. Fisher. 1989. High pp60^{c-src} level in human platelet dense bodies. *Blood.* 73:1545-1551.

Resh, M. D., and R. L. Erikson. 1985. Highly specific antibody to Rous sarcoma virus src gene product recognize a novel population of pp60^{v-src} and pp60^{c-src} molecules. *J. Cell. Biol.* 100:409-417.

Riabowol, K., G. Draetta, D. V. Brizuela, and D. Beach. 1989. The cdc2 kinase is a nuclear protein that is essential for mitosis in mammalian cells. *Cell.* 57:393-401.

Rohrschneider, L. R. 1979. Immunofluorescence on avian sarcoma virus-transformed cells: localization of the src gene product. *Cell.* 16:11-24.

Rohrschneider, L. R. 1980. Adhesion plaques of Rous sarcoma virus-transformed cells contain the src gene product. *Proc. Natl. Acad. Sci. USA.* 77:3514-3518.

Shalloway, D., P. M. Coussens, and P. Yaciuk. 1984. Overexpression of the c-src protein does not induce transformation of NIH 3T3 cells. *Proc. Natl. Acad. Sci. USA.* 81:7071-7075.

Shenoy, S., J. K. Choi, S. Baprodia, T. D. Copeland, J. L. Maller, and D. Shalloway. 1989. Purified maturation promoting factor phosphorylates pp60^{c-src} at the sites phosphorylated during fibroblast mitosis. *Cell.* 57:763-774.

Sobue, K., and K. Konda. 1988. Localization of pp60^{c-src} in growth cone of PC12 cells. *Biochem. Biophys. Res. Commun.* 157:1383-1390.

Tamura, T., R. R. Friis, and H. Bauer. 1984. pp60^{c-src} is a substrate for phosphorylation when cells are stimulated to enter cycle. *FEBS (Fed. Eur. Biochem. Soc.). Lett.* 177:152-156.

Virtanen, I., P. Ekblom, and P. Laurila. 1980. Subcellular compartmentalization of saccharide moieties in cultured and malignant cells. *J. Cell. Biol.* 85:429-434.

Warren, S. L., and W. J. Nelson. 1987. Non mitogenic morphoregulatory action of pp60^{v-src} on multicellular epithelial structures. *Mol. Cell. Biol.* 7:1326-1337.

Warren, S. L., L. M. Handel, and W. J. Nelson. 1988. Elevated expression of pp60^{c-src} alters a selective morphogenetic property of epithelial cells *in vitro* without a mitogenic effect. *Mol. Cell. Biol.* 8:632-646.

Willingham, M. C., G. Jay, and I. Pastan. 1979. Localization of avian sarcoma virus src gene product to the plasma membrane of transformed cells by electron microscopic immunocytochemistry. *Cell.* 18:125-134.